CAIT-UTC-NC52

Residual Capacity of Impacted Bridge Piers

FINAL REPORT
September 2019

Submitted by:

Andrew Sorensen, Ph.D.
Assistant Professor

Marvin Halling, Ph.D.
Assistant Professor

Ikwulono Unobe, Ph.D.
Post Graduate Researcher

Suman Roy, M.S.
Graduate Research Assistant

Department of Civil and Environmental Engineering
Utah State University
4110 Old Main Hill
Logan UT 83422-4110

External Project Manager
Rhett Arnell
Utah Department of Transportation
4501 South 2700 West
Salt Lake City, UT 84114

In cooperation with

Rutgers, The State University of New Jersey
And
U.S. Department of Transportation
Federal Highway Administration (FHWA)

Disclaimer Statement

The contents of this report reflect the views of the authors, who are responsible for the facts and the accuracy of the information presented herein. This document is disseminated under the sponsorship of the Department of Transportation, University Transportation Centers Program, in the interest of information exchange. The U.S. Government assumes no liability for the contents or use thereof.

The Center for Advanced Infrastructure and Transportation (CAIT) is a National UTC Consortium led by Rutgers, The State University. Members of the consortium are the University of Delaware, Utah State University, Columbia University, New Jersey Institute of Technology, Princeton University, University of Texas at El Paso, Virginia Polytechnic Institute, and University of South Florida. The Center is funded by the U.S. Department of Transportation.

1. Report No.	2. Government Accession No.	3. Recipient's Catalog No.
CAIT-UTC-NC52		

4. Title and Subtitle	5. Report Date
Residual Capacity of Impacted Bridge Piers	August2020
	6. Performing Organization Code CAIT/Utah State University

TECHNICAL REPORT STANDARD TITLE PAGE

7. Author(s)	8. Performing Organization Report No.
Suman Roy, Ikwulono Unobe, Andrew D. Sorensen, and Marvin Haling	CAIT-UTC-NC52

9. Performing Organization Name and Address	10. Work Unit No.
Department of Civil and Environmental Engineering Utah State University 4110 Old Main Hill Logan UT 83422-4110	11. Contract or Grant No. DTRT13-G-UTC28

12. Sponsoring Agency Name and Address	13. Type of Report and Period Covered
Center for Advanced Infrastructure and Transportation Rutgers, The State University of New Jersey 100 Brett Road Piscataway, NJ 08854	Final Report 12/15/2017 – 7/31/19
	14. Sponsoring Agency Code

15. Supplementary Notes
U.S. Department of Transportation/OST-R
1200 New Jersey Avenue, SE
Washington, DC 20590-0001

16. Abstract
The FHWA has recently initiated research to determine the vulnerability of bridge piers subject to vehicular impact. Vehicular impact to bridge piers results in varying levels of damage and corresponding reduction in structural capacity. The extent of the damage determines the level of corrective maintenance required to keep the bridge in service or the decision to take the bridge off-line for pier replacement. The majority of the existing studies in this area have taken a risk management approach in an attempt to limit the number of accidental occurrences. The majority of approaches rely on the assignment of a damage level index to determine suitability for continued service. However, these approaches do not take into consideration the reduction in capacity and ability of the pier to withstand additional hazard loading conditions such as seismic. These sequential hazardous loading conditions are not currently considered in existing design codes and as such the analysis assumes that each member has its design capacity when it experiences the hazard loading. This study seeks to identify the reduction in capacity that bridge piers experience as a function of vehicular impact to develop reduction factors that can be used in the reliability analysis of subsequent, post impact, hazard analysis.

17. Key Words	18. Distribution Statement
Bridge Piers, Vehicle Impact, Residual Capacity	

19. Security Classification (of this report)	20. Security Classification (of this page)	21. No. of Pages	22. Price
Unclassified	Unclassified	97	

Form DOT F 1700.7 (8-69)

Acknowledgments

The authors would like to thank the financial support given by the Office of the Assistant Secretary for Research and Technology of the United States Department of Transportation (USDOT OST-R) (Grant No: DTRT13-G-UTC28) to perform this research.

Table of Contents

List of Figures vii

List of Tables viii

Executive Summary 1

CHAPTER 1 Introduction 3

1.1. Problem Statement 3
1.1 Objective and Scope 4
1.2 Report Organization 4

CHAPTER 2 Literature Review and Existing Model Analysis 6

2.1 Introduction 6
2.2 Code Overview 7
2.2.1 Impact Mechanism 7

2.3 Vehicle Impact 13
2.3.1 Impact Behavior of the Columns and Possible Damage Modes 13
2.3.2 Vehicular Impact Models 14
2.3.3 Column Capacity Models 22

2.4 Collision Risk Analysis 27
2.4.1 Risk Acceptance Criteria 27
2.4.2 Collision Risk Model 28
2.4.3 Vessel Traffic Distribution 28
2.4.4 Probability of Aberrancy (PA) 29
2.4.5 Probability of Collapse (PC) 29

2.5 Damage Assessment 30
2.5.1 Collapse of Reinforced Concrete Column due to Dynamic Impact 30
2.5.2 Impact Damage Computation 33

2.5.3 Damage Index 34

2.6 Conclusions 38

CHAPTER 3 Reliability and Sensitivity Analysis of Vehicle Impacted RC Bridge Pier 40

3.1 Introduction 40
3.2 Reliability Analysis 40
3.3 Probabilistic Analysis of Pier under Impact 42
3.3.1 Representative Pier 42
3.3.2 Reliability Analysis 44
3.3.3 Load Model 45
3.3.4 Resistance Model 46
3.3.5 Sensitivity Analysis 50

3.4 Results 51
3.4.1 Assessment of Reliability 51
3.4.2 Sensitivity Analysis 53

3.5 Conclusions 57

CHAPTER 4 Residual Capacity of Vehicle Impacted RC Bridge Pier 59

4.1 Introduction 59
4.2 Materials 61
4.3 Methodology 62
4.3.1 Frontal Impact of Bridge Pier 62
4.3.2 Determination of Damage Index 65
4.3.3 Computation of the Residual Strength of Damaged Pier 66

4.4 Results 68
4.4.1 Analysis Parameters 68
4.4.2 Residual Capacity of Pier after Impact 68
4.4.3 Relationship between Pier Parameters and Residual Capacity 71

4.5 Conclusions 77
CHAPTER 5 Conclusions 78

5.1 Summary of Conclusions 78
5.2 Future Research 79

List of Figures

Figure 2-1 Model of Bending Stresses from Kinetic Energy 20

Figure 2-2 Support Conditions and External Load Applications for Example Pier 33

Figure 3-1 (a) Representative RC Bridge Pier, (b) Section A-A 43

Figure 3-2 Representative RC Bridge Pier 43

Figure 3-3 Probability of Failure of RC Pier due to vehicle impact at different velocities 53

Figure 3-4 Reliability indices for the RC pier at changing design parameters 54

Figure 3-5 Sensitivity of RC pier to External and Core Diameters 56

Figure 4-1 Pier Cross Section 62

Figure 4-2 Impact Pressure Diagram on the RC Bridge Pier 63

Figure 4-3 Relationship between Dynamic Impact and Vehicle Speed for Different Vehicle Masses 69

Figure 4-4 Residual Pier Axial Capacity at Different Vehicle Speeds 70

Figure 4-5 Residual Pier Shear Capacity at Different Vehicle Speeds 70

Figure 4-6 Vehicular Momentum and Residual Axial Capacity of Pier 72

Figure 4-7 Vehicular Momentum and Residual Shear Capacity of Pier 72

Figure 4-8 Relationship between Dynamic Impact and Pier Load Ratios 73

Figure 4-9 Damage Indices with the Pier Capacity Ratio 73

Figure 4-10 Relationship between Shear Reinforcement Pitch and Residual Axial Capacity 74

Figure 4-11 Relationship between Shear Reinforcement Pitch and Residual Shear Capacity 74

Figure 4-12 Residual Pier Capacity with the Corresponding Damage Indices 77

List of Tables

Table 2-1 Resultant Equivalent Static Forces for Impact Scenarios..... 21

Table 3-1 Design Variables and Corresponding Uncertainty Parameters 52

Table 3-2 Sensitivity of Each Design Parameter to the Limit State 55

Table 4-1 Damage Index Level Compared to Residual Pier Capacity 76

Executive Summary

The FHWA has recently initiated research to determine the vulnerability of bridge piers subject to vehicular impact. Vehicular impact to bridge piers results in varying levels of damage and corresponding reduction in structural capacity. The extent of the damage determines the level of corrective maintenance required to keep the bridge in service or the decision to take the bridge off-line for pier replacement. The majority of the existing studies in this area have taken a risk management approach in an attempt to limit the number of accidental occurrences. The majority of approaches rely on the assignment of a damage level index to determine suitability for continued service. However, these approaches do not take into consideration the reduction in capacity and ability of the pier to withstand additional hazard loading conditions such as seismic. These sequential hazardous loading conditions are not currently considered in existing design codes and as such the analysis assumes that each member has its design capacity when it experiences the hazard loading. This study seeks to identify the reduction in capacity that bridge piers experience as a function of vehicular impact to develop reduction factors that can be used in the reliability analysis of subsequent, post impact, hazard analysis.

Using a standard pier detail utilized by the Utah Department of Transportation, existing methods available in the literature are used to evaluate the damage indices and to compare those results to safety factors in current design codes. The reliability of the pier section is then determined as a function of material properties, geometry, vehicle mass, and vehicle impact velocity. Using numerical analysis techniques, the pier is also analyzed to determine the residual axial and shear capacity post-impact. Finally, the residual capacity is used to determine reduction factors that correlate to damage indices that can be used in future evaluation.

The results of the analysis show that current design codes are non-conservative for vehicle impact design especially for large mass vehicles such as semi-tractor trailers. Results from the reliability analysis indicate probabilities of failure of the pier ranging from 45% to 80% for a vehicle at different velocities from 25 mph to 80 mph. Sensitivity analyses are undertaken to understand the relationship between the individual design variables and the corresponding reliability. Results show that increasing the diameter of the pier without changing other design parameters will result in a lower reliability index and higher probability of failure for the pier. The opposite is true for changing the transverse reinforcement while keeping other parameters unchanged. The underlying relationship between the external and core diameters is also explored to understand how the relationship between these variables affect the system reliability.

From the results of the residual capacity analysis, it is determined that increasing the steel ratio, reducing the pitch of the transverse reinforcement and using a higher grade concrete along with larger pier diameter will help the pier better resist vehicular impact. Furthermore, it is also expected that the pier will perform better against dynamic shear if the shear reinforcement diameter is increased in order to reach higher steel grade. Finally, a relationship between damage indices and residual capacity of the pier has been established and can be used to better analyze the damage and corresponding condition of the damaged pier.

CHAPTER 1 Introduction

1.1. Problem Statement

The FHWA has recently initiated research to determine the vulnerability of bridge piers subject to vehicular impact. Vehicular impact to bridge piers results in varying levels of damage and corresponding reduction in structural capacity. The extent of the damage determines the level of corrective maintenance required to keep the bridge in service or the decision to take the bridge off-line for pier replacement. The majority of the existing studies in this area have taken a risk management approach in an attempt to limit the number of accidental occurrences. However, little research has been carried out to evaluate the damage levels resulting from intentional impact. Furthermore, even less has been done to understand the residual loading capacity of bridge piers post impact. Unlike accidental impact, intentional impact results in higher levels of damage due to the acceleration of the vehicle at the time of impact.

In the case of intentional impact with terroristic intent, additionally loading subsequent to the initial impact damage may occur immediately due to a fire or explosion. This multi-hazard loading condition has the capability to cause severe damage to bridge piers and cause major disruptions to critical transportation networks. Current multi-hazard loading analysis techniques rely on fault tree analysis techniques, which do not take into account a possible reduction in capacity from the initial loading. Recently, the PI has utilized a different approach, the resistance reduction method, to include a reduced capacity in post-impacted piers. However, there is little to no information available on the post-impact capacity of the bridge piers and as such adequate reduction factors are required to accurately predict probabilities of failure due to multi-hazard loading. This project seeks to determine a predictive methodology for calculating capacity reduction values for vehicular impacted bridge piers. Additionally, the contribution of

each component (i.e. concrete and reinforcement) within the bridge pier is analyzed via sensitivity analysis for their contribution to residual capacity.

1.1 Objective and Scope

The objective of the research is to identify the reliability of vehicular impacted bridge piers as a function of their residual capacity and ability to withstand loading post-impact. The three specific objectives of this research correspond to the report chapters and are as follows:

1) Identify the current state of the practice for the evaluation of post impacted reinforced concrete bridge piers and use this information to analyze a typical bridge pier section.

2) Analyze and identify the reliability of reinforced concrete bridge piers subject to vehicle impact and a function a material properties, geometry, vehicle mass, and vehicle impact velocity.

3) Analyze a typical pier section to correlate the residual axial and shear load capacity as a function of material properties, geometry, vehicle mass, and vehicle impact velocity.

4) Correlate residual axial and shear capacity to existing damage level indices.

1.2 Report Organization

This report is organized as follows:

- Chapter 2 provides a summary of the current state of the practice concerning the evaluation, analysis, and numerical modelling of the behavior of reinforced concrete bridge piers and columns. A review of the current codes used in impact resistant bridge pier design is also presented. A typical pier section is used to demonstrate the evaluation process.
- Chapter 3 derives a numerical analysis technique to determine the reliability of reinforced concrete bridge piers subject to vehicle impact. Sensitivity analysis is then utilized to

determine the relationship between material properties, geometry, vehicle mass, and vehicle speed to identify which factors provide higher levels of contribution to reliability and conversely which factors provide devastating to the in place serviceability of the piers.

- Chapter 4 presents a numerical analysis technique to determine the axial and shear load residual capacities post vehicle impact. These results are used to draw a correlation with existing damage level indices in order to provide resistance reduction factors for additional loading reliability analysis.
- Chapter 5 summarizes the research conclusions and discussion of work moving forward.

CHAPTER 2 Literature Review and Existing Model Analysis

2.1 Introduction

The increasing occurrence of vehicle-pier collision accidents have raised significant questions about the safety of bridge structures leading to an uptick in studies on the structural health of bridge piers affected by such impact events in recent years. Some collision accidents result in severe damage to bridge structures, such as pier fracture and bridge collapse, while others result in less severe, cosmetic, damage such as concrete cracking at the impact location. To study and understand the behavior and failure modes of damaged piers, it is necessary to accurately analyze the bridge-pier failure pattern.

Bridge piers, lower story columns of buildings, traffic signal structures, and electric poles are the structural members most vulnerable to vehicular impact. A rise in structural collision cases has been reported in the USA as well as in other parts of the world. A review of the causes of bridge failures in the United States from 1966 to 2005, shows the frequency of occurrence of bridge failures from different causes in the United States. Analyzing bridge failures over this 38-year period, it was found that 15% of the failures could be attributed to vehicular collisions, making this the second most likely cause of bridge failure. Comparatively, earthquakes, which are of great concern and have received considerate attention in designing bridges, only account for about 1% of failures. Overall, 200 bridges of the 1502 cases of failed bridges studied, collapsed due to collision (Knott and Prucz, 2003).

Even more common are accidents where vessels collide with bridges causing significant damage but not necessarily a collapse of the structure. A study of river towboat collisions with bridges located on the U.S. inland waterway system during the short period from 1970 to 1974 revealed that there were 811 accidents with bridges costing $23 million in damages and causing

14 fatalities. On average, 35 vessel collision incidents are reported every day to U.S. Coast Guard Headquarters in Washington, D.C (Deng et al., 2015).

With few guidelines available for designing structures resistant to dynamic actions resulting from sudden vehicular collisions with structural members, structural designers have to rely on computer simulations from specialist software to make design decisions. However, there is some concern with verifying the results and consequently the design decisions based on these results. This study is an attempt to collate the research on vehicular collisions on the serviceability of reinforced concrete (RC) bridge piers to help develop more concise guidelines for the design of bridge structural members' resistance to impact loads from vehicle collision as well as to provide guidance on evaluating post impacted piers.

This chapter is organized in the following manner: first a brief overview of the existing design codes' approach to designing impact safe structures, followed by a discussion of the state of the art with respect to vehicular as well as boat (barge) impact on bridge piers. The following sections focus on an appraisal of models developed to characterize the different aspects of impact scenarios, including a new model as an aggregation of impact forces from different studies to better represent the different variables present in an impact scenario.

2.2 Code Overview

2.2.1 Impact Mechanism

The cost associated with protecting a bridge from catastrophic vehicular collision can be a significant portion of the total bridge cost and must be included as one of the key planning elements in establishing a bridge's type, location, and geometry (AASHTO, 2012). One method of protecting the structural members of the bridge is designing the structural member to directly withstand collision forces. For such designs, accurately defining the vehicular impact load on RC

members is very important in properly understanding the response and behavior of the structural member to impact events (Consolazio et al., 2005). However, the current analysis methods and experimental procedures used to estimate the capacity of, and demand on, RC columns do not capture the complex mechanism of an impact event, thus reducing the efficiency of these designs.

Pioneering work on understanding the impact scenario between moving vehicles and reinforced concrete piers was carried out by Meir-Dornberg in 1983. The series of theoretical and experimental studies carried out for both dynamic and static loading conditions resulted in relationships that characterized the impact scenario between barges and reinforced concrete piers (Meir-Dornberg, 1983). These relationships, shown in Equations 2.1 to 2.3, form the basis for the AASHTO guide specifications for barge impact loads.

$$a_B = 10.2\left(\sqrt{1+\frac{C_H E_B}{5672}}-1\right).\frac{1}{R_B} \tag{2.1}$$

$$P_B = \begin{cases} 4112 a_B R_B & a_B < 0.34 \\ (1349 + 110 a_B) R_B & a_B \geq 0.34 \end{cases} \tag{2.2}$$

$$R_B = \frac{1}{35} B \tag{2.3}$$

Where: E_B is the initial kinetic energy of barge (k-ft), a_B is the barge deformation in ft., B is the barge width (ft.), P_B is the barge impact force (kips), R_B is the modification factor to correlate the impact force for the barge having width ≠ 35 ft (10.7 m), and C_H is the hydrodynamic mass coefficient for the surrounding water upon the moving barge.

To account for vehicle collisions, the AASHTO code requires that the abutments and piers located within a distance of 9.144 m (30.0 ft.) of the edge of the roadway be designed for an equivalent static force of 2,669 kN (600 kips), assumed to act in a direction of 0 to 15° to the

edge of the pavement in a horizontal plane at a height of 1.542 m (5.0 ft.) above the ground. A similar format of design impact load stipulations for structures vulnerable to collision on a highway have been adopted by major codes of practice around the world including the United Kingdom, Japan, Australia, and Germany (AASHTO, 2012; CEN, 2004; Standards Association of Australia, 2004). However, several studies and computer simulations have shown this static force to be inadequate especially for impact scenarios involving large vehicles and/or high speeds (Remennikov and Kaewunruen, 2007; Tsang and Lam, 2008). The uncertainties associated with using this static force in designing for impact is exacerbated by a failure to consider variables such as vehicle mass, its impact velocity, as well as pier characteristics in estimating this value (Auyeung, 2019).

The AASHTO Guide Specification provides examples and contains a relatively extensive discussion of various types of physical protection systems, such as fenders, pile-supported structures, dolphins, protective islands, and floating structures (AASHTO, 2012). However, the code does not include specific procedures and recommendations for the actual design of such protection structures. Thus, further research is needed to establish consistent analysis and design methodologies for protecting structures, particularly since these structures undergo large plastic deformations during the collision. Integral to this is the development of a definitive load model that will accurately detail the load transfer mechanism from a vehicle to a bridge pier during impact. Boat/Barge Impact

Worldwide, in the period from 1960 to 1998, there were 30 major bridge collapses due to vehicular collisions, resulting in 321 casualties. The greatest loss of life took place in 1983 when a passenger ship collided with a railroad bridge while attempting to transit through a side span of the bridge over the Volga River in Russia. A hundred and seventy-six people were reported dead

in the ensuing collision, most occurring when a packed movie theater on the top deck of the passenger ship was sheared off by the low vertical clearance of the bridge superstructure. Fifteen of the reported bridge accidents within that period occurred in the United States, including the 1980 collapse of the Sunshine Skyway Bridge crossing Tampa Bay in Florida in which 396 meters of the main span collapsed and 35 lives were lost as the result of an empty 35,000 DWT bulk carrier colliding with the bridge (Knott and Prucz, 2003).

More recently, a major collision occurred in Portland Maine, when a loaded tanker rammed into the guide pile fender system of the Million Dollar Bridge over the Ford River resulting in extensive damage to the bridge as well as an environmental mishap when 170,000 gallons of oil spilled into the river. Although the main cause of the accident was attributed to pilot error, a contributing factor was certainly the limited horizontal clearance of the navigation opening through the bridge (only 29 meters or 95.14 feet) (Michel and Winslow, 2000).

A number of factors affect the vulnerability of a bridge to vessel collision including waterway geometry, water stage fluctuations, current speeds, weather conditions, vessel characteristics, navigation conditions, bridge size, location, and geometry as well as the efficiency of existing bridge protection systems. Serious collisions between vessels and bridges are extreme events associated with a great amount of uncertainty, especially with respect to the impact loads involved. Since designing for the worst-case scenario could be overly conservative and economically undesirable, a certain amount of risk must be considered as acceptable. The commonly accepted design objective is to minimize (in a cost-effective manner) the risk of catastrophic failure of a bridge component, and at the same time reduce the risk of vessel damage and environmental pollution. To adequately design for the vulnerabilities listed, several considerations are taken into account including selection of a bridge site to minimize the

presence of structural components in proximity to areas traversed by vehicular traffic as well as adequate horizontal and vertical clearance. Analysis of past collision accidents show that bridges with a main span less than two to three times the design vessel length or less than two times the channel width are particularly vulnerable to vessel collision. To avoid collisions with the superstructure, the vertical clearance below the navigation span is usually based on the highest vessel that uses the waterway in a ballasted condition and during periods of high water levels (Larsen, 1993). Such clearance requirements need to take into consideration site-specific data on actual and projected vessels and must be coordinated with the Coast Guard in the United States. General data on vessel height characteristics are included in the design of the reference approach spans.

Bridge protection measures can be included in the design of bridges deemed to be at risk from vehicular collisions to avert damage from such incidences. These measures include designing a pier fender system to reduce impact loads, increasing span lengths to locate piers out of reach of large vessels, and using physical protection systems around structural members to bear the brunt of collisions, can be used to prevent the occurrence of collisions. These options are usually evaluated and the most cost-efficient system selected for use on bridge projects. Designing an effective crash barrier system requires an in depth understanding of the load transfer mechanisms occurring during impact events (Woisin, 1979).

The estimation of the load on a bridge pier during a ship collision is a complex problem. The actual force is time dependent and varies depending on the type, size, and construction of the vessel, its velocity, the degree of water ballast in the forepeak of the bow, the geometry of the collision, and the geometry and strength characteristics of the bridge. As a result, there is a very

large scatter in the collision force values recommended in different vessel collision guidelines or used in various bridge projects (Knott and Prucz, 2003).

Ship collision forces are commonly applied as equivalent static loads. Based on the several barge-pier collision studies, carried out over nine years (1967-1976), to protect nuclear reactors from ship collisions, Woisin (1979) proposed an empirical relationship correlating the average impact force averaged over time, $\bar{P}(t)$, and the mean impact force averaged over the damage depth, $\bar{P}(a)$, as shown in Equation 2.4.

$$\bar{P}(t) = 1.25\bar{P}(a) \tag{2.4}$$

Utilizing Woisin's data, AASHTO proposed another empirical relationship for bulk carriers for the speed range of 8 to 16 knots, as shown in Equation 2.5, and Equation 2.6 for speed beyond this range (AASHTO, 2012):

$$P_s = 220(DWT)^{1/2}(V_i/27) \tag{2.5}$$

$$P_s = 0.98(DWT)^{1/2}(V_I/16) \tag{2.6}$$

Where: DWT is the dead weight tonnage in metric tons, V_i is the vessel velocity in ft/sec, and P_s is the mean impact force in kips.

It can be seen from Equations 2.5 and 2.6 that accurate estimation of the maximum possible velocity and deadweight tonnage of vessels is very important in obtaining the correct design impact load due to ship collisions.

The contribution of the superstructure to the transfer of loads to adjacent substructure units depends on the capacity of the connection of the superstructure to substructure and the relative stiffness of the substructure at the location of the impact. Analysis guidelines for determining the distribution of collision loads to adjacent piers can be found in (Knott and Prucz, 2003). To determine how much of the transverse impact force is taken by the pier and how much is

transferred to the superstructure, two analytical models are typically used. One is a two-dimensional or three-dimensional model of the complete pier and the other is a two-dimensional model of the superstructure projected on a horizontal plane (Knott and Prucz, 2003).

2.3 Vehicle Impact

Some vehicle collisions and resulting accidents cause severe damage to bridge structures, such as pier fracture and bridge collapse, while others caused slight damage to the piers, such as concrete cracking at the impact location. Vehicle collision design is commonly based on equivalent static loads that include global forces for checking overall capacity and local forces for checking local strength of bridge components.

2.3.1 Impact Behavior of the Columns and Possible Damage Modes

Data from full-size vehicle-pier collision tests conducted using a 36.3-ton (72.60 kips) truck to collide with a steel column of diameter of 900 mm (35.4331 in) at 80 km/hr. (49.71 miles/hr.), led to the suggestion of 2669 kN (600.013 kips) as the design impact force for vehicle collision (Buth et al., 2011). The current AASHTO-LRFD bridge code provisions assume this constant value for the shear force demand on a column subject to vehicle impact. However, the actual shear force demand imposed on a column is typically larger than the AASHTO-LRFD prediction and is not a constant value but rather dependent on a number of variables including the vehicle velocity and mass (Feyerabend, 1988).

Drop hammer tests to analyze the effect of reinforcement ratios on the dynamic response and damage levels on RC beams, as well as their impact behavior without stirrups, and using fiber reinforcement, have been carried out in different studies (Kishi et al., 2001; Kulkarni and Shah, 1998; Banthia et al., 1989). Saatci and Vecchio (2009) conducted four groups of drop hammer impact tests on RC beams to study the effects of shear capacity on the impact behavior

of RC beams and developed simplified single degree of freedom methods for impact analysis of structures. Although several important results were obtained from these studies, it is difficult to extrapolate these results directly for bridge piers as the impact tests were mainly required to be carried out to study the impact behavior and dynamic shear capacity of RC beams (Zhou et al., 2017). Differences in the impact location and boundary conditions between beams and piers will result in dissimilar behaviors between these structural elements regardless of similarities in loading. The impact location of beams is at the mid span, while the impact location of piers is 1 foot above the bottom; beams seldom bear axial load, while piers always carry the weight from the bridge superstructure and vehicles.

To study behaviors and failure modes of the damaged piers, it is necessary to accurately analyze the peak impact force, the maximum deformation, impact force, and deformation time histories of the piers. These variables are also helpful when designing protection schemes for piers subject to vehicle collision.

2.3.2 Vehicular Impact Models

The alternative equal energy method is used in modeling barriers that can be used as physical protection systems for bridge piers. This method relies on fundamental energy methods to develop the design equations. Equations in Annex C of Euro-code 1 for horizontal "hard impact" scenarios are based on this principle as shown in Equation 2.7 (CEN, 2004).

$$1/2\, mv_0^2 = 1/2\, k\Delta^2 \tag{2.7}$$

Where: m is the mass of impactor, v_0 is the cruising velocity, k is the stiffness of the linear elastic system, Δ is the impact induced deflection of the target, and F is the equivalent static force to match the displacement demand.

Rearranging Equation 2.7 to determine the equivalent static force (F), yields Equation 2.8.

$$F = k \cdot \Delta = v_0/[k \cdot m]^{1/2} \quad (2.8)$$

Equations 2.7 and 2.8 are derived for the design of vehicular barriers by equating the kinetic energy of the moving vehicle with the energy absorbed by the deforming target (the barrier). A similar method of calculation is used to predict the maximum force imposed by the colliding vehicle into a rigid concrete profiled barrier. In this case, the initial kinetic energy is assumed to be dissipated entirely by the vehicle. In both cases, the energy absorption is assumed to be entirely taken up by only one element of the impact (i.e. either the impacting vehicle or the target) (Remennikov and Kaewunruen, 2007). Equations 2.7 and 2.8 are also well known and easy to use with both the impactor and the structural system (target) idealized into respective connected lumped masses. Using these equations, the impact action of a vehicle on a bridge pier, or vehicular parapet, on a highway is represented by a prescribed equivalent static load. This simple format of quantifying impact action as an equivalent static force (ESF) is convenient for structural design purposes.

Although this method of estimating an equivalent static force (ESF) to replace the expected dynamic load occurring during impact does take into consideration the deformation of the impacted pier, it does not consider possible inertial effects which may play a role in structural resistance to dynamic loads (Auyeung at al., 2019). Consequently, the extent to which this equivalent static force provisions can be adapted for the design and analysis of a diverse array of impact scenarios remains uncertain (Lam, 2017).

To establish an impact load model that includes parameters specific to the impact scenario, Zhou and others utilized the equivalent displacement method to convert the peak impact force into an equivalent static force to be used as an estimate of the impact force acting over the duration of

the impact scenario. The developed model based on the peak impact force (PIF) and the instantaneous displacement occurring during impact is shown in Equation 2.9 (Zhou et al., 2018).

$$ESF = \int_0^t p(i)d(i)\,di/d_{max} \quad (9)$$

Where: p(i) is the instantaneous impact force, t is the impact duration, di is the instantaneous deformation, $d_{\max}$ is the maximum deformation, and i is the instantaneous moment.

Comparing results obtained from simulations using this model to the suggested design impact loads in different standards, the study showed that the different standards severely underestimated the possible impact force that will be generated in a collision between a vehicle and a reinforced concrete pier, especially in scenarios involving larger vehicles and/or higher impact velocities. This effectively demonstrated that the impact design forces in current standards are not conservative. It was also found that on average, the simulated peak impact forces were about 3.5 times larger than the ESF, meaning that even with the inclusion of a design safety factor (currently 1.5), a pier designed with current standards could be vulnerable to large impact events including heavy vehicle collisions (Zhou et al., 2017). As such, more study and insight is required to better define acceptable design parameters for impact loads.

Another study on the relationship between the different variables influencing the damage occurring during vehicular impact events, implied that the ESF obtained using the model shown in Equation 2.9 gave an estimate of the expected force from impact which is not conservative. This is due to the model not considering the duration of the impact, which is a critical component of the scenario (Zhou and Li, 2018). To overcome this perceived shortcoming, a modified global equivalent static force, which averages the integration of the collision process by the impact duration was suggested. The modified model is shown in Equation 2.10 (Zhou and Li, 2018).

$$\text{GESF} = \frac{\int_0^t p(i)di}{t} \tag{2.10}$$

Where: p(i) is the instantaneous impact force, t is the impact duration, di is the instantaneous deformation, and i is the instantaneous moment.

Although demonstrated to be adept at estimating an equivalent static force characteristic of the vehicle impact scenario, the GESF was considered to be unsuitable for this particular purpose (Zhou and Li, 2018). This is because averaging over the entire duration of the impact scenario deemphasized the effect of the peak impact force. As a result, while the GESF is quite adept at making accurate estimations of the ESF for long duration impact scenarios where the effect of the PIF is lessened over the impact duration, it fails to accurately portray the behavior of shorter-term impact scenarios. To better capture the effects of both the PIF and impact duration, the study suggested a modification to the GESF. Designated the local equivalent static force (LESF), this modification involved integrating the impact force over a 50 millisecond window around the force and then averaging by 50 milliseconds (Zhou and Li, 2018). By limiting the integral to a shorter window, the effect of both the time frame and the PIF on the impact scenario are adequately included in the model, localizing the effect of the impact force to a shorter range of time it is expected to have occurred in. The 50-millisecond window was selected with reference to the 50-millisecond moving average often used to in extrapolating the impact time history curve in vehicle crash analyses (Buth et al., 2011). The revised model (LESF) is as shown in Equation 2.11 (Zhou and Li, 2018).

$$\text{LESF} = \frac{\int_{t_p-25}^{t_p+25} p(i)di}{50} \tag{2.11}$$

Where: t_p is the time pf the peak impact force (PIF).

A computation of the ESF for a vehicle-pier impact scenario using the above models requires a knowledge of the time history curve of the impact scenario. According to the structural dynamic theory (Chopra, 2006), the vehicle–pier collision system can be simplified into an un-damped system and a half-sine impulse can be taken as the impact impulse, as shown in Equation 2.12 (Zhou and Li, 2018).

$$p(i) = P \sin\left(\frac{\pi i}{t}\right) \tag{2.12}$$

Where: P is the peak impact force (PIF), and t is the total duration of the impact.

Experimental work as well as finite element analyses (FEA) can be used to determine the PIF (Abdelkarim and El Gawady, 2017). However, that is a very complicated process requiring accurate modeling of both the impacting vehicle and the bridge pier system in question.

An alternative approach to calculating the ESF is a stiffness based approach as utilized in (El-Tawil et al., 2005). This approach defines the ESF as the static force required to produce displacement equal to that of the maximum displacement occurring from the vehicle collision at the point of impact. A similar approach recommended by Eurocode-1 for computing the ESF utilizes both the expected displacement of the pier and the vehicle alongside its impacting kinetic energy to estimate the ESF as shown in Equation 2.13 (CEN, 2002).

$$EC_{ESF} = \frac{KE}{\delta_c + \delta_d} \tag{13}$$

Where: KE is the vehicle's kinetic energy, m is the vehicle's mass, v_r is the vehicle's velocity, δ_c is the vehicle deformation (calculated as the change in length between the vehicle nose and the center of mass according to NCHRP 350 (Abdelkarim and El Gawady, 2017)), and δ_d is the column deformation (the lateral displacement of the column at the point of impact load).

Although not requiring knowledge of the peak force to estimate the ESF, an inability to generalize for all possible scenarios due to the inclusion of vehicle specific characteristics as well as case specific deformation information obtainable only after sophisticated simulations in computing the ESF, limits the Euro code model.

An alternative model, modeled off the results of simulations correlating the peak of the twenty five millisecond moving average (PTMSA) to the kinetic energy of the impacting vehicles, was proposed by (Abdelkarim and El Gawady, 2017). This approach primarily utilizes the mass and velocity of an impacting vehicle in computing the ESF, thus removing the dependence of other models on specific simulations to estimate some variables required in computing the ESF. This model termed the kinetic energy equivalent static force (KEB_{ESF}) is as shown in Equation 2.14.

$$KEB_{ESF} = 33\sqrt{mv_r^2} = 46\sqrt{KE} \tag{2.14}$$

Where: m = the vehicle mass in ton, v_r = the vehicle velocity in m/s, and KE = kinetic energy of the vehicle in kN.m.

The PTMSA in particular was used in developing this model as several simulations by the authors showed it best estimated the impact force developed in a vehicle impact scenario and accurately predicted the resultant condition of the pier post impact (Abdelkarim and El Gawady, 2017). In simplifying the model for computing an equivalent static force, only the mass and impact velocity are used in computing the KEB_{ESF}. As such, this model does not consider the possible effects of other variables such as pier size and geometry on the resulting impact force. These variables do however have a telling effect on the resultant impact force from a vehicle-pier collision Consolazio et al., 2002).

Some of the models suggested by researchers and reproduced above require knowledge of the peak impact force from a crash scenario in estimating the final design equivalent static

force. However, such values are only available after actual impact tests or simulations and are a function of a number of variables which are unique to specific crash scenarios. To overcome this shortcoming, a model is developed using test data from several published studies (Zhou and Li, 2018; Cao et al., 2019; Mohammed and Parvin, 2013; Gomez and Alipour, 2014) to extrapolate a relationship between the peak impact force and kinetic energy of the impacting vehicle. Due to the variations in geometric dimensions of the different piers used in the different studies, and the effect such variations have on the peak impact force, the resulting peak impact forces were normalized to bending stresses in developing the model. This allows the model to be used in estimating the peak impact force irrespective of the geometric dimensions of the pier in question. Figure 2-1 shows the developed model obtained via a regression analysis of the results (line of best fit) from the different studies.

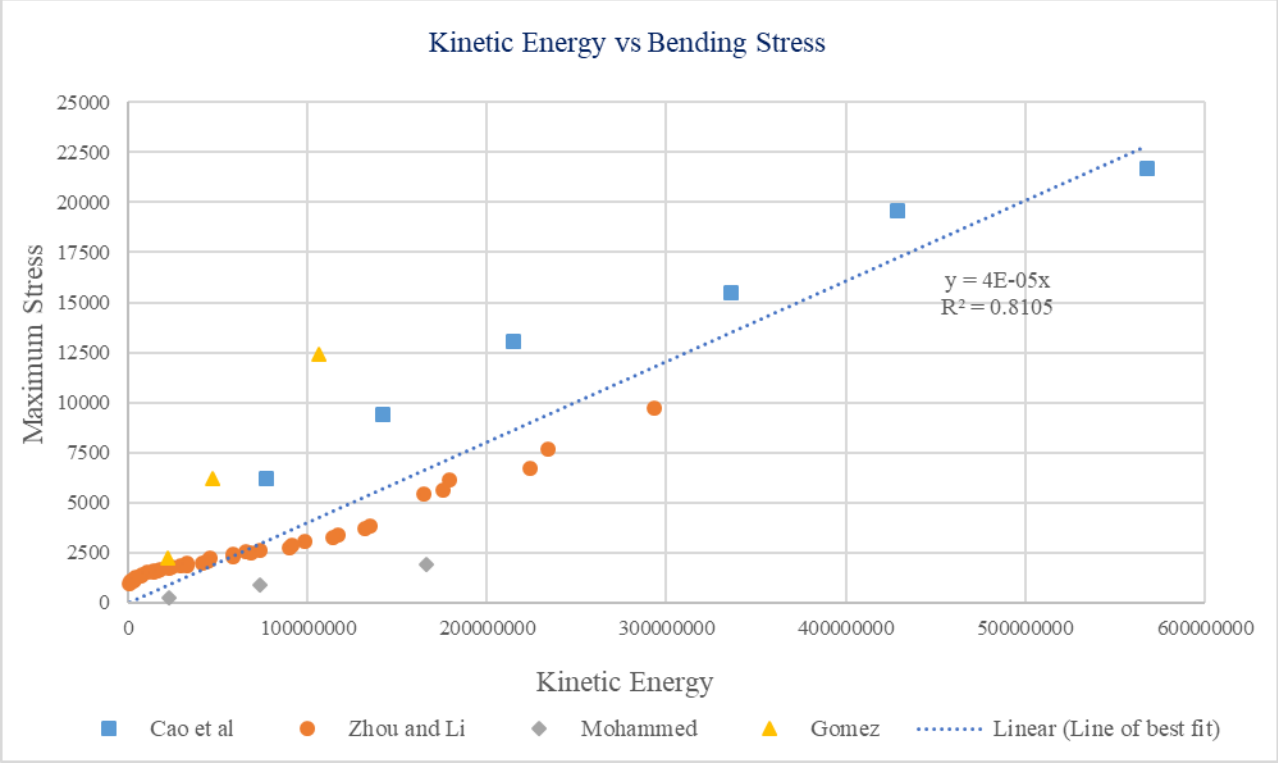

Figure 2-1 Model of Bending Stresses from Kinetic Energy

In developing this model, the bending stress resulting from the peak impact force was used in lieu of using the force directly. This was done in order to capture the effect of the pier geometry in the model, allowing for the inclusion of these variables in estimating the peak impact force that will result in an impact scenario and beyond that, the equivalent static force that will accurately encapsulate the impact of a vehicle on a RC pier. From the regression, a model for estimating the peak impact force is developed and shown in Equation 2.15.

$$P = (4 * 10^{-5}E) * \frac{4I}{(L*c)} \tag{2.15}$$

Where: E is the kinetic energy, absorbed by the impacted column, I is the moment of inertia of the column, L is the height of the column and c is the perpendicular distance from the neutral axis of the cross section to the farthest point on the cross section of the column.

The results of a comparison between the different models for estimating the ESF is shown in Table 2-1. This comparison is made using data collected from low velocity impact experiments carried out using a single mass and changing velocities (Zhang et al., 2018).

Table 2-1 Resultant Equivalent Static Forces for Impact Scenarios

Peak Impact force (kN)	**Velocity (m/s)**	**GESF**	**LESF**	**KEB_{ESF}**
237.5	2	1663.974	28.09189	795.9982
250	2.47	1751.551	162.182	983.0578
325	2.83	2277.017	247.5612	1126.337
325	3	2277.017	1496.719	1193.997

From the results, it can be seen that there are large disparities in the estimated ESF values for impact scenarios using the different published models. This can be attributed to the different variables utilized in computing the ESF values. The GESF is based primarily on the value of the peak impact force and as such results in the most conservative values which are much higher that the peak forces. The LESF on the other hand, takes some other parameters of the impact scenario

such as the total duration of the impact and the time instant of the peak impact force in addition to the peak impact force. This results in the least conservative model albeit more characteristic of the expected behavior of the impact over its duration. The KEB_{ESF} is a middle ground value between the two models based on the expected sinusoidal behavior of the impact scenario. This model, based only off the mass and velocity of the impacting vehicle is a more convenient method of estimating the ESF. However, this method does not incorporate the intrinsic characteristics of the impact scenario which are very distinct for each impact incident.

2.3.3 Column Capacity Models

The dynamic shear force capacity of an RC column and the demand imposed on it during impact depends both on the structural properties as well as on loading conditions. Therefore, it is necessary to understand the behavior of the column during impact in order to accurately estimate its shear force capacity. An accurate estimate of the dynamic shear force capacity and the dynamic shear force demand is necessary to ensure that the structural capacity is kept above the demand. This ensures the structure withstands possible vehicle impact events and remains stable (Feyerabend, 1988).

A number of experiments have been conducted to understand the failure mechanism and dynamic effects during vehicle impact. Some significant observations made in these experiments include the following:

- Cracks propagate through the aggregate thickness, thus increasing the strength and toughness of the concrete member.
- In concrete, the brittle behavior increases with the increase in loading rate (material).
- The strength of the reinforcing steel bar increases with loading rate (material) (Lam, 2017).

- Shear failure mode becomes predominant with increasing loading (system).
- A plastic hinge is formed at the point of contact (system).

Reinforced concrete (RC) columns with inadequate transverse reinforcement are vulnerable to shear failure especially from impact. For RC columns without adjacent load redistribution members around them, severe damage by shear from either impact or other external factors leading to a deterioration in the axial load carrying capacity can lead to a global or partial structural collapse. It is therefore necessary to evaluate the residual axial load carrying capacity, to ensure proper post impact evaluation, and adequate repairs or retrofitting. Shear strength provisions have been implemented in various design codes following a number of experimental studies carried out to investigate the shear strength mechanism in structural members. Most design codes are based on concrete strength and transverse reinforcement strength to determine the shear capacity of reinforced concrete sections. These two components are simply added together to provide the full shear capacity of the section in the presence of flexure and axial force.

No guidelines are available for estimating the dynamic shear force capacity and the demand on the RC column subject to vehicle collision (Sharma et al., 2014). The analysis and design methods specified in design codes do not account for variations in the damage state and the required performance levels. In light of this, it is necessary to define a standard procedure to estimate the dynamic shear force capacity of the RC column and to estimate the dynamic shear force demand imposed on it corresponding to different performance levels and impact scenarios. A possible method to do this is using the modified compression field theory El-Tawil et al., 2005).

Based on the Compression Field Theory, the Modified Compression Field Theory (MCFT) was developed after testing different reinforced concrete member elements subjected to pure shear, pure axial load, and a combination of shear and axial load (Vecchio and Collins, 1986). The MCFT model is able to accurately predict the shear behavior of concrete members subjected to shear and axial forces (Rasheed et al., 2004). However, the MCFT is a relatively complex analysis method. A simplified version of the theory called the Simplified Modified Compression Field Theory (SMCFT) was developed to predict shear strength with a relatively simpler procedure and similarly accurate results (Bentz et al., 2006). Several approaches based on SMCFT have been developed for estimating the shear capacity as described in the following sections.

Priestley and others (1994) proposed a model for the shear strength of reinforced concrete members under cyclic lateral loading as the summation of strength capacities of concrete (V_c) and steel (V_s) and an arch mechanism associated with axial load (V_P) as expressed in Equations 2.16 to 2.18 (Rasheed et al., 2004, Cowper and Symonds, 1957).

$$V = V_c + V_s + V_p \tag{2.16}$$

$$V_c = k(f_c' A_e)^{1/2} \tag{2.17}$$

$$V_s = \pi \cdot A_h \cdot f_{yh} \cdot D' \cdot \cot(\theta) \tag{2.18}$$

Where: k within plastic end regions depends on the member's ductility, $A_e = 0.8A_g$, D' is the spiral or hoop diameter, A_h is area of a single hoop/spiral, f_{yh} is the yield stress of spiral steel and θ is the angle of the critical inclined flexure-shear cracks to the column axis, taken as θ = 30°, unless limited to larger angles.

A_e is the effective shear area of a circular column with diameter D and is computed as shown in Equation 2.19.

$$A_e = 0.8A_g \tag{2.19}$$

The shear strength enhancement (V_p) resulting from axial compression is considered to be a variable and is given by Equation 2.20.

$$V_p = P \cdot \tan \alpha_{cs} = (D - c) \cdot P/2\alpha_{cs} \quad (2.20)$$

Where: D is the diameter of the circular column, c is the depth of the compression zone, and P is the shear span. For a cantilever column, α_{cs} is the angle formed between the column axis and the strut from the point of load application to the center of the flexural compression zone at the column plastic hinge critical section.

Standard New Zealand (Ghee et al., 1989) developed equations based on a 45- degree truss model for the nominal shear strength of concrete columns. In determination of V_c within the plastic hinge zone, the longitudinal steel amount and the axial load effect are considered. However, the axial load effect is applied only if the axial load ratio exceeds 0.1. If the axial load ratio is less than or equal to 0.1, the concrete contribution to shear strength is ignored. The shear strength carried by concrete is thus calculated using Equation 2.21.

$$V_c = (0.001 + 1.45A_s/bs) \cdot (f_c')^{1/2} \cdot \left[P/f_c' \cdot A_g - 0.1bd\right]^{1/2} \quad (2.21)$$

Where: A_s is the area of transverse reinforcement within spacing s, and b is the width of the column. For circular columns, b is taken as the column diameter D.

The shear strength carried by transverse reinforcement is based on analysis of effective shear resistance provided by transverse hoops assuming a 45- degree truss mechanism using Equation 2.22 (Ghee et al., 1989).

$$V_s = \left[\pi \cdot A_{sp} \cdot f_{yh} \cdot D_{sp}\right]/2s \quad (2.22)$$

Where: A_{sp} is the cross-sectional area of transverse steel, D_{sp} is the core diameter of the circular section defined by the center-to-center diameter of transverse steel, f_{yh} is yield stress of transverse steel, and s is vertical distance between transverse steel.

Committee 426, a joint ASCE and ACI committee on shear strength of concrete members, produced a nominal design shear strength (V_n) equation based on the additive model as shown in Equation 2.23 (Rasheed and Abouelleil, 2015).

$$V_n = V_c + V_s \tag{2.23}$$

Where: V_c and V_s are critical and transverse shear strength distribution for steel, respectively.

The committee did not consider the influence of ductility when estimating total shear strength of circular columns (Priestly et Al, 1994). The shear strength carried by concrete (V_c) is calculated using Equations 2.24 and 2.25 (ASCE, 2013).

$$V_c = v_b\left[1 + 3P/\left(f_c' A_g\right)\right]A_e \tag{2.24}$$

$$v_b = (0.0096 + 1.45\rho) \cdot (f_c')^{1/2} \leq 0.03(f_c')^{1/2} \ \ ksi \tag{2.25}$$

Where: v_b is the nominal concrete shear stress, and ρ is the longitudinal tension steel ratio. The longitudinal tension steel ratio is calculated in terms of the gross area of the column. In order to calculate the transverse steel shear strength contribution (V_s), the committee assumed a diagonal compression strut model at 45° to the member longitudinal axis in developing the relationship shown in Equation 26.

$$V_s = \pi/2 \cdot A_h \cdot f_{yh} \cdot D'/s \tag{2.26}$$

Where: D' is the spiral or hoop diameter and A_h is the area of a single hoop or spiral.

The ACI 318-11 (2011) code considers a portion of the design shear force to be carried by the concrete shear resistance (V_c), and the remainder by transverse steel (V_s), both of which are added together for the total design shear force as shown in Equations 2.27 to 2.29 (ASCE, 2011).

$$V = V_c + V_s \tag{2.27}$$

$$V_s = \left[A_v f_{yt}(sin\alpha_i + cos\alpha_i)\right]d_s/s \tag{2.28}$$

$$V_c = 0.002\left[1 + P/2000A_g\right] \cdot \mu \cdot (f_c')^{1/2} \quad (2.29)$$

Where: P_a is the axial load the section is subjected to, A_g is gross cross-sectional area, f_c' is concrete compressive strength, b is the width of the section, d is the effective depth of the section, A_v is the area of transverse reinforcement within the spacing (s), f_{yt} is the yield stress of transverse steel, α_i is the angle between the inclined stirrups and the longitudinal axis of the member, and μ is a modification factor to account for lightweight concrete.

2.4 Collision Risk Analysis

2.4.1 Risk Acceptance Criteria

Bridge components exposed to vessel collision are subjected to a wide range of impact load scenarios. Due to economic and structural constraints, bridge design for vessel collision is not based on the worst-case scenario and a certain amount of risk is considered acceptable (Knott and Prucz, 2003). The risk acceptance criteria consider both the probability of occurrence of a vessel collision and the consequences of the collision. The probability of occurrence of a vessel collision is affected by factors related to the waterway, vessel traffic, and bridge characteristics. The consequences of a collision depend on the magnitude of the collision loads and the bridge strength, ductility, and redundancy characteristics.

The AASHTO (2012) provisions specify an annual frequency of bridge collapse of 0.0001 for critical bridges and an annual frequency of bridge collapse of 0.001 for regular bridges. These annual frequencies correspond to return periods of bridge collapse equal to 1 in 10,000 years, and 1 in 1000 years, respectively. Critical bridges are defined as those bridges that are expected to continue to function after a major impact because of social/survival or security/defense requirements.

2.4.2 Collision Risk Model

Various collision risk models have been developed to attain design acceptance criteria. In general, the occurrence of a collision is separated into three events: (1) a vessel approaching the bridge becomes aberrant, (2) the aberrant vessel hits a bridge element, and (3) the bridge element that is hit fails (Sharma et al., 2012). Collision risk models consider the effects of the vessel traffic, the navigation conditions, the bridge geometry with respect to the waterway, and the bridge element strength with respect to the impact loads and are generally expressed as shown in Equation 2.30.

$$AF = (N)(PA)(PG)(PC)(60.1) \tag{2.30}$$

Where: AF is the annual frequency of collapse of a bridge element, N is the annual number of vessel transits (classified by type, size, and loading condition) which can strike a bridge element, PA is the probability of vessel aberrancy, PG is the geometric probability of a collision between an aberrant vessel and a bridge pier or span, and PC is the probability of bridge collapse due to a collision with an aberrant vessel.

The variables expressed in Equation 2.30 are discussed in the following sections.

2.4.3 Vessel Traffic Distribution

The number of vessels, N, passing the bridge based on size, type, and loading condition and available water depth is determined individually for each pier and span component to be evaluated. All vessels of a given type and loading condition are divided into discrete groupings of vessel size by DWT (dead weight tonnage) to determine the contribution of each group to the annual frequency of bridge element collapse (AASHTO, 2012).

Once the vessels are grouped and their frequency distribution is established, information on typical vessel characteristics may be obtained from site-specific data or from published

general data such as the AASHTO Guide Specifications and Commentary for Vessel Collision Design of Highway Bridges or Ship Collision with Bridges: The Interaction Between Vessel Traffic and Bridge Structures (AASHTO, 2012; Sharma et al., 2012).

2.4.4 Probability of Aberrancy (PA)

The probability of vessel aberrancy, PA, is the likelihood of a vessel being out of control near a bridge. Such loss of control may occur as a result of pilot error, mechanical failure, or adverse environmental conditions. The probability of aberrancy is primarily related to the navigation conditions at the bridge site. Vessel traffic regulations, vessel traffic management systems, and navigation aids can be used to improve the navigation conditions and reduce the probability of aberrancy.

The probability of vessel aberrancy can be evaluated based on site-specific information including historical data on vessel collisions, ramming, and groundings in the waterway and vessel traffic, navigation conditions, and bridge/waterway geometry. This has been done for various bridge design provisions and specific bridge projects worldwide, with probability of aberrancy values ranging from $0.5*10^{-4}$ to $7.0*10^{-4}$.

As an alternative, the AASHTO provisions recommend base rates for the probability of vessel aberrancy which are adjusted using correction factors for bridge location relative to bends in the waterway, currents acting parallel to vessel transit path, crosscurrents acting perpendicular to vessel transit path, and the traffic density of vessels using the waterway. The recommended base rates are $0.6*10^{-4}$ for ships and $1.2*10^{-4}$ for barges (Larsen, 1993).

2.4.5 Probability of Collapse (PC)

The probability of collapse, PC, is a function of many variables including vessel size and type, forepeak ballast and shape, speed, direction of impact, and mass. It is also dependent on the

ultimate lateral load strength of the bridge pier, particularly the local portion of the pier impacted by the bow of the vessel. Based on collision damages observed from numerous collision accidents between ships, an empirical relationship for the bridge-ship collision situation has been developed. This relationship based on the ratio of the ultimate pier strength (H) to the vessel impact force (P), is used to determine the probability of collapse (Knott and Prucz, 2003). For H/P ratios less than 0.1, PC varies linearly from 0.1 at H/P = 0.1 to 1.0 at H/P =0.0. For H/P ratios greater than 0.1, PC varies linearly from 0.1 at H/P = 0.1 to 0.0 at H/P = 1.0.

2.5 Damage Assessment

2.5.1 Collapse of Reinforced Concrete Column due to Dynamic Impact

The analysis of a RC column subjected to impact was conducted to evaluate its dynamic behavior based on quasi-static conditions (Tsang and Lam, 2008). The analysis, considering a typical element at position x (measured from the mid-point) of the column, the internal forces acting on the element (lateral shear force Q and the bending moment M) as well as the external force acting on the element in the transverse direction, proposed the equations of motion of the elements as shown in Equations 2.31 to 2.33 (Tsang and Lam, 2008).

$$\partial Q/\partial x + m\ddot{w} = f(x,t) \tag{2.31}$$

$$\partial M/\partial x - Q = 0 \tag{2.32}$$

$$f(x,t) = \begin{cases} \frac{F(t)}{c} \; when \; |x| \le c/2 \\ 0 \; when \; |x| > c/2 \end{cases} \tag{2.33}$$

Where: w is the transverse deflection, m is the mass of the beam per unit length, and c is the length of the contact surface between vehicle and concrete column, assumed to be 0.2 m (0.656 feet).

Conversely, the impact force F(t) would be equal to the frontal stiffness of the impacting vehicle, K, multiplied by the shortening of the vehicle, u, based on the linearity assumption as shown in Equation 2.34.

$$F(t) = Ku \tag{2.34}$$

Eliminating the shear force Q from Equations 2.31 and 2.32 yields Equation 2.35.

$$\partial^2 M/\partial x^2 + m\ddot{w} = f(x,t) \tag{2.35}$$

Note that the rotational inertia of the column cross-section is ignored, as it is expected to have little effect on the global dynamic behavior of the column (Tsang and Lam, 2008).

The reinforced concrete column employed in this study has a uniform rectangular cross-section and the constitutive relationships between bending moment, M, and curvature, κ, are assumed to be elastic-perfectly plastic, and are written in Equations 2.36 and 2.37.

$$M = \begin{cases} EI\kappa \ when \ 0 < \kappa \leq \kappa_e \\ M_u \ when \ \kappa > \kappa_e \end{cases} \tag{2.36}$$

$$\kappa = \partial^2 w/\partial x^2 \tag{2.37}$$

Where: E is the Young's modulus of the material, 'I' is the second moment of area of the cross-section, M_u is the ultimate bending moment of the column, and κ is the maximum elastic curvature.

It is further observed that the total duration of the impact is around $50*10^{-3}$ s, and hence, the corresponding strain rate is in the order of 0.1 s^{-1}. For this rate of loading, the dynamic effect, known as the high strain rate effect, significantly enhances the strength and ductility of reinforced concrete.

Figure 2-2 shows a reinforced concrete column, axially loaded and restrained at both ends from rotation and translation under an impact load used in simulating the response behavior of a reinforced concrete column to dynamic impact loads (Thilakarathna et al., 2010). On application

of a triangular load pulse, the displacement of the column increases with the load until it reaches its peak, at which point the displacement decreases steadily albeit with some small increases in the post peak region until the residual displacement is achieved. This behavior is characteristic of the axial load acting on the column, which develops second order bending effects. In an actual impact event, there could be some contact losses due to the relative movement of the bodies in this region as the speed of the deformation of the column exceeds the velocity of the vehicle even though both are moving in the same direction. As such, failure due to vehicle impact digresses from the typical failure in flexure under mid span impact. Consequently, a conventional hypothesis based on the energy absorption capacity of the column may not be applicable for the resultant response of the column to impact loads as the energy absorption characteristics mainly depend on the flexural deformation of the column. Since the column is not subjected to flexural deformations, a small portion close to the impact region experiences highly localized stress and absorbs an excessive amount of energy. This localized stress may exceed the yield stress of the concrete, leading to abrupt deformation of the column during impact. This will considerably reduce the effective area of the column and the resultant eccentricity of the axial load diminishes the axial load carrying capacity of the column. Under these circumstances, the column fails initially in shear and subsequently in flexure, leading to collapse. The decisive failure modes can be categorized as shear and shear-flexural types of failures depending on the test variables as observed during simulations (Thilakarathna et al., 2010).

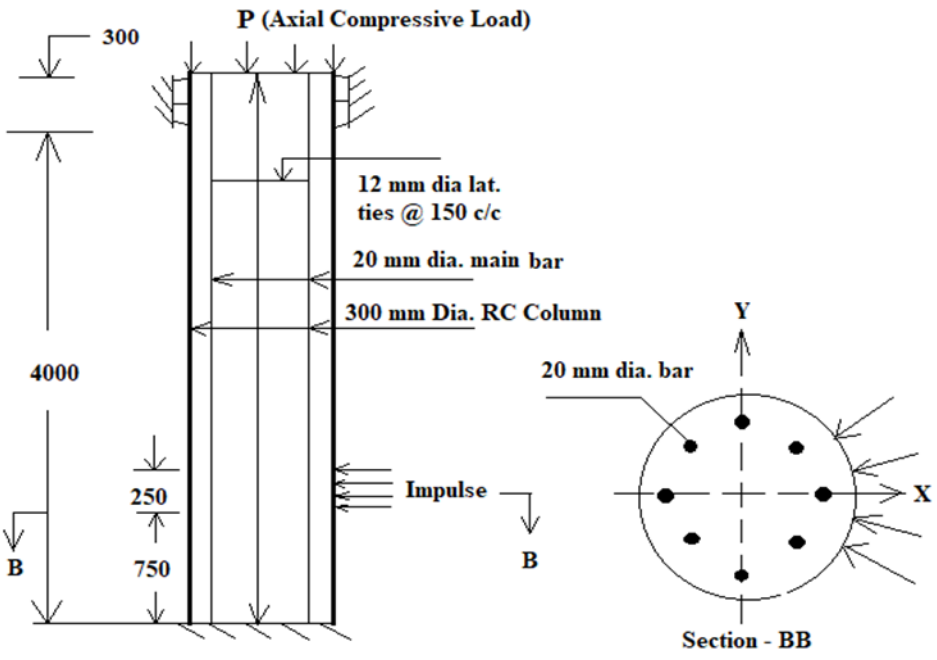

Figure 2-2 Support Conditions and External Load Applications for Example Pier

2.5.2 Impact Damage Computation

During vehicle impact, the RC column sustains different levels of damage depending on the geometry, material properties, and boundary conditions of the column and the velocity and type of vehicle. To categorize damage and delineate the operational state of the impacted pier, three performance levels have been defined to be based on the observable damage which may have occurred during impact (Bo and Daofan, 2011). The damage levels increase in intensity from insignificant damage to total collapse of the column and the corresponding performance levels are defined as follows: fully operational with no damage (P_1), operational structure with damage (P_2), and total collapse of structure (P_3). The severity of the impact scenario varies depending on the type of vehicle and its velocity. Intensity of the impact can be grouped in three categories according to the severity: low (L), medium (M), and high (H) based on the weight and the velocity of the vehicle.

This damage classification process relates low (L) impact intensity with the structure remaining fully operational (P_1), medium (M) intensity with the structure being operational with damage (P_2) and high (H) intensity impact with total collapse (P_3). Using these performance levels to define the damage state of an impacted pier requires the determination of a limit state criterion for use in estimating the damage to the pier and by extension, its performance level. Different researchers have utilized different limit state criteria to estimating damage (Abdelkarim and El Gawady, 2017; Agrawal et al., 2013). However, this method of damage estimation is qualitative and cannot be used to comprehensively determine the residual axial capacity of the pier in question after the impact has occurred.

Alternatively, the damage occurring during impact is appraised using a damage index. Computed as a ratio of the impact load to the capacity of the impacted pier, these damage indices have recently been proposed for use as a quantifiable measure of the ensuing damage to a RC pier after an impact event (Remennikov and Kaewunruen, 2007; Zhou and Li, 2018).

2.5.3 Damage Index

The quantification of the damage occurring from a vehicle collision with a pier can be made using the damage index (Baker et Al, 2012). Computed as a damage ratio between the structural capacity and demand from the impact, the damage index quantifies the damage and as such, better elaborates the state of the impacted pier. The damage index is divided into the tensile damage index d_t and compressive damage index d_c, which are represented by Equations 2.38 and 2.39.

$$d_t = 0.999/D\left[(1+D)/\left\{1+De^{-C(\tau_t-\tau_{0t})}\right\}-1\right] \tag{2.38}$$

$$d_c = d_{max}/B\left[(1+B)/\left\{1+Be^{-A(\tau_c-\tau_{0c})}\right\}-1\right] \tag{2.39}$$

Where: τ_t and τ_c are tensile energy and compressive energy for concrete material, respectively, τ_{0t} and τ_{0c} are tensile damage threshold and compressive damage threshold

for concrete material, respectively, and d_{max} is the maximum damage index. The parameters A and B or C and D are used for setting the shape of the softening curve plotted as stress displacement or stress-strain.

A simplified method of estimating the damage index to predict the estimated damage expected to occur on a pier during an impact event is the use of a relationship between the kinetic energy, shear capacity and pier diameter. This relationship, developed as a ratio between force demand and capacity is as shown in Equation 2.40 (Auyeung et al., 2019).

$$Damage\ Ratio = \frac{\frac{kinetic\ energy\ (kJ)}{\emptyset V_C(kN)}}{Pier\ diameter\ (m)} \tag{40}$$

Although adequately expressing the damage index as a ratio between the demand on, and capacity of, the impacted column, this relationship relies solely on the kinetic energy of the impacting vehicle for the force demand. As such, the resulting index may not be a true reflection of the state of the pier as other variables which will have an effect on the resulting force demand during impact are neglected.

An alternative method used in computing the damage index is a ratio of the equivalent static force to the shear capacity of the pier. Shown in Equation 2.41, this method allows for the computation of the damage index (λ) irrespective of the method used in estimating the ESF (Zhou and Li, 2018).

$$\lambda = I_{dyn}/V_{dyn} \tag{2.41}$$

Where: I_{dyn} is the vehicle equivalent static force and V_{dyn} is the dynamic shear.

Concrete and steel exhibit an increase in strength capacity when placed under high rates of loading (Auyeung et Al, 2019). This phenomenon is a function of the strain rate effect on the reinforced concrete. As a result, the dynamic shear capacity of reinforced concrete (V_{dyn}) is determined using both the nominal shear capacity and a dynamic increase factor (DIF) to account for this increase

in strength. Malvar recommended a relationship for calculating the DIF in terms of the quasi strain rate. These relationships as shown in Equations 2.42 to 2.44 holds true for strain rates between 10^{-4} s^{-1} and 225 s^{-1} (Malvar, 1998).

$$DIF = \left(\frac{\dot{\varepsilon}}{10^{-4}}\right)^{\xi} \tag{2.42}$$

$$\xi = 0.019 - 0.009(\sigma_{dyn}/60) \tag{2.43}$$

$$\sigma_{dyn} = [1 + (\dot{\varepsilon}/C)^{1/P}] \cdot (\sigma_p + \beta E_p \varepsilon_{eff}) \tag{2.44}$$

Where: $\dot{\varepsilon}$ is the strain rate, ξ is a constant which depends on the dynamic yield stress of steel at the strain hardening zone, σ_{dyn} is the dynamic yield stress of steel, σ_o is the initial yield stress, ε_{eff} is the equivalent plastic strain, E_p is the plastic hardening modulus, β is the hardening parameter, $\dot{\varepsilon}$ is the quasi-static strain rate, and parameters C and P are constants. Alternatively, according to CEB (1990), the increase in peak stress in concrete, or the dynamic impact factor (DIF), can be calculated using Equation 2.45 (Malvar, 1998).

$$\text{DIF} = (\dot{\varepsilon}/\dot{\varepsilon}_s)^{1.026\alpha'} \text{ for } \dot{\varepsilon} \leq 30s^{-1} \tag{2.45}$$

Where: $\dot{\varepsilon}$ is the strain rate, $\dot{\varepsilon}_s$ is the quasi-static strain rate that equals 30 *10^{-6} s^{-1}, and α' is defined in Equation 2.46 (Malvar, 1998).

$$\alpha' = 1/(5 + 9\, f_c/f_{co}) \tag{2.46}$$

Where: f'_c is the concrete peak stress and f_{co} is set at 1.45 ksi (10 MPa) and hence, the DIF for the purposes of this study would be in the order of 1.3.

Residual strength of RC column using DIF in terms of concrete also presents significant information though concrete has less contribution than steel during impact. The dynamic shear, V_{dyn}, the dynamic impact factor, and shear capacity of the column, V_n, are related by the relationship in Equation 2.47.

$$V_{dyn} = V_n \cdot (DIF) \tag{2.47}$$

Where: DIF is the dynamic impact factor, and V_n is the shear capacity of the reinforced concrete column with spiral transverse shear reinforcement.

Calculated damage indices fall between 0 and 1 with 0 indicating no damage and 1 indicating complete collapse of the pier. The severity of damage is scaled as follows: λ = 0-0.2 is low damage, 0.2-0.5 is medium damage, 0.5-0.8 is high damage, and 0.8-1 is collapsed and no longer in service [48]. Depending on the severity of the damage to the column, the column could be retrofitted and returned into service if only minimally damaged, or totally replaced if the severity ranges from highly damaged to fully collapsed. Using the computed damage index, the residual capacity of the RC pier can be determined, thus removing the ambiguity of classifying impact damage by visual inspection. The relationship between the damage index and residual strength of the damaged column is shown in Equation 2.48 (Shi et Al, 2008).

$$\lambda = 1 - (P_{N,residual}/P_{N,design}) \tag{2.48}$$

Where: $P_{N,\,residual}$ is the residual strength of the damaged column after vehicular impact and $P_{N,\,design}$ is the design axial load carrying capacity of the undamaged reinforced concrete bridge pier as stated in ACI.

Rearranging Equation 2.48 allows for the determination of the residual strength of the damaged RC pier as shown in Equation 2.49 (ASCE, 2013; ACI, 2011).

$$P_{N,residual} = (1 - \lambda) \cdot P_{N,design} \tag{2.49}$$

Computing the residual strength of the pier allows for accurately ascertaining the expected response of a structural member to an impact force, thus cutting down on the cost of physical experimentation. The computation of a damage index which considers both the structural capacity

and expected impact load, allows for the accurate computation of the residual strength and thus improving the accuracy of post damage assessment of a RC pier.

2.6 Conclusions

In reinforced concrete (RC) structures, columns are usually the most vulnerable members to collisions. However, the existing design guidelines and provisions for protection of these members against vehicle collisions are not adequate. In particular, the desired behavior and the associated performance levels of a structure during a vehicle collision are not well defined. Therefore, there is a need to assess the vulnerability of existing structures against such collisions and proffer solutions to limit such vulnerabilities.

This presentation and adaptation of the existing literature in this chapter attempts to provide a comprehensive insight into developed methodologies, and studies aimed at characterizing the damage sustained by RC bridge piers after collisions with vehicles. Various performance-based studies are examined for an ideal method to identify the intensity of damage. In addition, an attempt at categorizing different failure patterns according to severity is presented in which specific damage levels due to localized action of impact along with surface concrete spalling are correlated to different performance levels.

Based on the numerical analysis results from several studies, the current impact design provisions of AASHTO and Euro-code are deemed to be un-conservative, which could result in piers designed with the current standard codes being vulnerable to large impact energy. The recommended value of equivalent static force in the current standards seems to fall short of possible impact forces as they are not representative of the dynamic behavior of impact forces. Alternative methods proposed for determining the ESF are presented and a model to overcome

some of the perceived shortcomings of these methods was proposed. However, more study and insight is required for widespread application. Some salient details in this chapter are as follows:

1. An equivalent static force model to predict impact forces arising from vehicular collisions with RC bridge piers is proposed.
2. Axially loaded columns and their shear impact design using different approaches are discussed with emphasis on the dynamic effect.
3. Performance based studies of the impacted columns are presented and explained.

CHAPTER 3 Reliability and Sensitivity Analysis of Vehicle Impacted RC Bridge Pier

3.1 Introduction

This chapter investigates the reliability of a post impact bridge pier, proposing a model for estimating the probability of failure (Ayyub and McCuen, 2016) based on characteristics peculiar to the impact scenario including the speed of impact, mass of the vehicle, and geometric and material parameters of the RC pier. Accordingly, the paper discusses:

a. The probability of failure and attendant reliability indices of a RC bridge pier subjected to vehicular impact scenarios computed via alternative methodologies.
b. The sensitivity of several design parameters to the reliability of the bridge pier and;
c. The influence of uncertainty in the design parameters to the design capacity of the pier i.e. a comparison of the probabilistic analytical procedure to the more generally used deterministic procedure.

3.2 Reliability Analysis

The reliability of a structure is stated as its ability to meet the demands required of it over a defined period of time (Nowak and Collins, 2012). The reliability or otherwise of a structural member or system can be inferred from the design parameters used in developing the system or member parameters. However, these parameters are not deterministic in nature but are rather random variables subject to variability in their specifications. As such, there is no certainty that the resulting structural member will completely fulfil the design criteria. Reliability analysis is a process of determining the effect of these parameter uncertainties on the performance of the design elements and system as a whole with a view to minimizing the possibility of failures occurring.

Structural systems (bridges, buildings etc.) and their constituent components are designed to be load resisting systems. These systems are usually unique in layout and/or consist of very expensive components, thus negating the possibility of determining their reliability via experimentations of full-scale tests. Consequently, their reliabilities are appraised from predictive models using probabilistic methods which take into account the uncertainties of the constituent parameters (Netherton, 2012). Antipodal to the reliability of structures or structural systems, failure, the inability of the structure to meet its design requirements can also be determined using the reliability performance function. This function describes the performance of the component in meeting the demand for a defined scenario (Ayyub and McCuen, 2016). Exceedance of the capacity or resistance in the function by the load or demand component results in a failure and vice versa. Mathematically, probability of failure is modelled as shown in Equation 3.1 comprising limit state function (Nowak and Collins, 2012).

$$P_f = Pr[g(x) < 0] \tag{3.1}$$

Where: P_f is the probability of failure, g(x) is a performance or limit state function and x is a vector of all the random variables included in the limit state function.

The limit state function in the probability model encapsulates the design parameters and their attendant uncertainties for both the load (demand) component and the resistance (capacity) component of the structural system. In this study, the damage index model is used in developing the limit state model to capture both the demand from vehicular impact and the shear capacity expected to absorb this dynamic demand.

3.3 Probabilistic Analysis of Pier under Impact

3.3.1 Representative Pier

In order to analyze the serviceability and residual strength of the circular reinforced concrete (RC) bridge-pier, and its behavior during and immediately after vehicular impact, a representative circular pier specimen (Figure 3-1) is analyzed. The specifications for the RC bridge pier are taken from the Utah Department of Transportation (Ameli and Pantelides, 2017). The pier is assumed to have a uniform circular cross-section over its entire length.

The representative pier is designed with a concrete grade of 3 ksi, longitudinal (primary reinforcement) grade 60 steel reinforcement (60 ksi tensile strength), and transverse grade 40 steel reinforcement (40 ksi tensile strength). The unrestrained length of the pier is taken as 8.6 feet with circular cross-section. Figure 3.1(b) shows the detail of the RC pier cross section. The pier has primary reinforcement of (6) #8 steel re-bars throughout till foundation with a spiral shear reinforcement by #4 steel (grade of 36 ksi) rebar @ 2-1/2 inches pitch throughout. Shear reinforcement provided in the pier conforms to the minimum shear reinforcement criteria (ACI, 2011). In addition, the representative pier also satisfies the shear reinforcement criteria to be provided in terms of rebar diameter, and pitch of spiral reinforcement as well (Furlong, 2014).

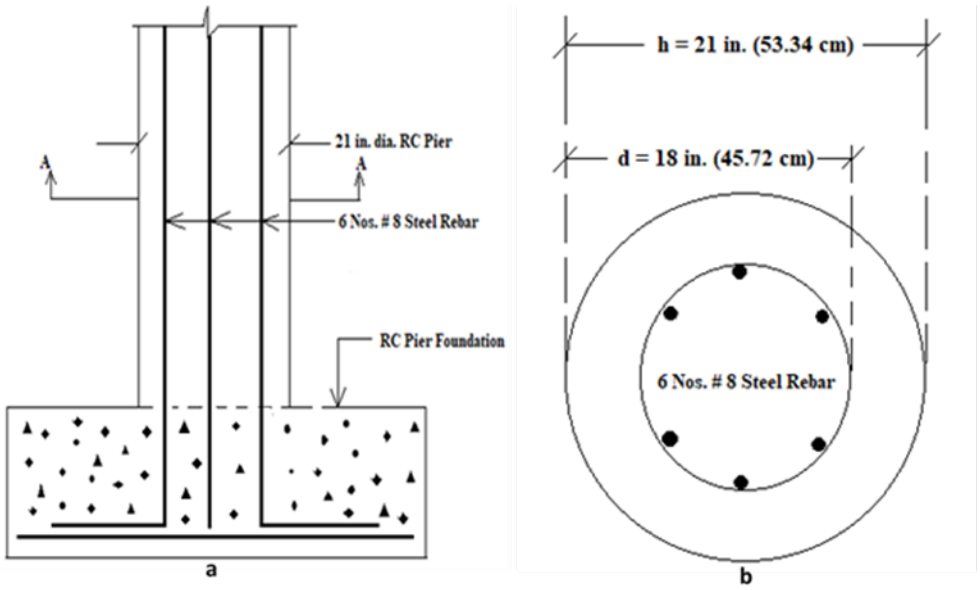

Figure 3-1 (a) Representative RC Bridge Pier, (b) Section A-A

Figure 3-2 Representative RC Bridge Pier

The reliability analysis comprises of utilizing several methods in determining the probability of failure and reliability indices as well as sensitivity analyses to determine which of the variables involved in the structural design of the pier are most involved in defining the outcome of the impact scenario.

3.3.2 Reliability Analysis

Any structural failure occurs when demand exceeds the capacity (Nowak and Collins, 2012). Vehicle collisions with bridge piers can result in varying levels of damage to the pier ranging from minimal damage to complete collapse. When exposed to dynamic impact from vehicular motion, reinforced concrete piers resist the impact primarily via their shear capacity (Abdelkarim and El Gawady, 2017). As such, the damage assessment of bridge piers from the vehicle impact principally involves an assessment of the degradation of the capacity post impact. This damage of reinforced concrete material under impact load is identified using some parameters from the impact scenario, coalesced into a single parameter known as the damage index. Characterizing the severity of damage to the structural member, the damage index (λ), is expressed as a ratio of the impact force and the dynamic shear capacity of the pier which are in turn contingent upon the vehicle characteristics and pier characteristics respectively. The damage index is computed using the expression shown in Equation 3.2 (Feyerabend, 1988):

$$\lambda = I_{dyn}/V_{dyn} \tag{3.2}$$

Where: I_{dyn} is the peak vehicle dynamic impacted force, and V_{dyn} is the dynamic shear due to impact.

The damage index is used to classify the severity of damage to the pier. Rated from 0 to 1, an increase in the index correlates to an increase in damage of the pier and vice versa. The dynamic shear capacity of the pier (V_{dyn}) is determined by considering the effect of strain rate on the characteristic material behavior of the structural member. This involves computing a dynamic impact factor for the material characteristics and impact strain rate as shown in (Cowper and Symonds, 1957; Mander et al., 1988). This impact factor is then multiplied by the design shear capacity to obtain the dynamic shear capacity.

Based on the damage index (λ), computed using the dynamic impact and dynamic shear capacity, the limit state ratio for this reliability study is defined as the exceedance of the shear capacity by the dynamic impact force exerted by the impacting vehicle. The derived limit state equation is as shown in Equation 3.3.

$$g(x) = 1 - \lambda = 1 - \frac{I_{dyn}}{V_{dyn}} \tag{3.3}$$

3.3.3 Load Model

The load model for the reliability analysis of the concrete pier under vehicular impact is encapsulated in the dynamic impact force exerted by the impacting vehicle. This dynamic impact force (I_{dyn}), is represented by the pressure from the impacting vehicle, the pier geometric dimensions and the duration of impact as shown in Equations 3.4, 3.5 and 3.6 (Vrouwenvelder, 2000; Zhou and Li, 2018).

$$I_{dyn} = \frac{\int_{t_d-0.025}^{t_d+0.025} I_r \sin\left(\frac{\pi t_d^+}{t}\right) di}{0.05} \tag{4}$$

$$I_r = (4 * 10^{-5} E) * \frac{4I}{(h*c)} \tag{5}$$

$$t = \sqrt{\frac{m}{k}} \tag{6}$$

Where: I_{dyn} represents the frontal shock due to impact, I_r, is the peak reflected pressure (overpressure), t represents the impact duration, E is the kinetic energy, absorbed by the impacted pier, I is the moment of inertia of the pier, h is the height of the pier, c is the perpendicular distance from the neutral axis of the cross section to the farthest point on the cross section of the pier, m is the mass of the impacting vehicle and k is the vehicle stiffness (Shi et al., 2008; Vrouwenvelder, 2000).

3.3.4 Resistance Model

Resistance models in reliability analyses are usually designed around material properties and geometric dimensions of the structural member under consideration. For an impact analysis, the primary resisting mechanism of the pier is its shear capacity.

As suggested in ASCE and ACI 318 the design shear capacity of the reinforced concrete pier is determined using Equation 3.7 (ACI, 2011; MacGregor et al., 2012).

$$V_{N,design} = V_c + V_s \tag{3.7}$$

Where: V_c is the shear strength carried by the concrete and V_s is the transverse shear capacity.

The shear strength, V_c, is computed as shown in Equation 3.8 (MacGregor et al.., 2012).

$$V_c = \nu_b[1 + 3P_{N,design}/f_c' \cdot A_g] \cdot A_e \tag{3.8}$$

Where: A_g represents the gross cross-sectional area of the concrete in the pier and A_e is 80% of A_g, i.e. A_e becomes $0.8A_g$, and ν_b is the shear constant.

The shear constant (ν_b) is determined using Equation 3.9 (MacGregor et al., 2012).

$$\nu_b = [0.0096 + 1.45\rho_t] \cdot (f_c')^{1/2} \leq 0.03(f_c')^{1/2} ksi \tag{3.9}$$

Where: ρ_t is the longitudinal steel ratio and $P_{n,\ design}$ represents the axial load capacity of the reinforced concrete pier.

Furthermore, the transversal shear capacity, V_s is calculated using Equation 3.10 (MacGregor et al., 2012).

$$V_s = \pi/2\, A_h \sigma_{yh}\, D'/s \tag{3.10}$$

Where: A_h is the area of a single hoop or spiral, D' is the spiral or hoop diameter, s denotes the pitch of the helix, and σ_{yh} represents the yield stress of transverse steel.

The dynamic shear, V_{dyn}, and shear capacity of the pier, V_n, are related by the relationship in Equation 3.11 (Feyerabend, 1988).

$$V_{dyn} = V_n \cdot (DIF) \tag{3.11}$$

Where: DIF is the dynamic impact factor, and V_n is the shear capacity of the reinforced concrete pier with spiral transverse shear reinforcement.

The dynamic impact factor (DIF) can be expressed in terms of quasi-static strain rate (έ) and is expressed as in Equation 3.12 (Mander et al., 1988).

$$DIF = \left(\frac{\acute{\varepsilon}}{10^{-4}}\right)^{\xi} \tag{3.12}$$

Where: έ is the strain rate and ξ is a constant which depends on the dynamic yield stress of steel at the strain hardening zone as expressed in Equation 3.13 (Feyerabend, 1988; Mander et al., 1988):

$$\xi = 0.019 - 0.009(\sigma_{dyn}/60) \tag{3.13}$$

έ is also used to scale the yield stress with the factors as shown in Equation 3.14 (ACI, 2011; Cowper and Symonds, 1957; Pacnik and Novak, 2010).

$$\sigma_{dyn} = [1 + (\acute{\varepsilon}/C)^{1/P}] \cdot (\sigma_p + \beta E_p \varepsilon^{eff}) \tag{3.14}$$

Where: σ_{dyn} is the dynamic yield stress of steel, σ_o is the initial yield stress, ε^{eff} is the equivalent plastic strain, E_p is the plastic hardening modulus, β is the hardening parameter, έ is the quasi-static strain rate, and parameters C and P are constants (ACI, 2011; Feyerabend, 1988).

The modulus of elasticity of the steel rebar at the strain hardening stage, E_P, is determined using Equation 3.15 (Mander et Al, 1988).

$$E_p = \sigma_P/\varepsilon_{eff} \tag{3.15}$$

From these equations, it can be surmised that the load model is based on the dynamic impact while the resistance model is based on the dynamic shear capacity of the pier. Both these models are made up of parameters which are random variables. The basic parameters defining a random variable are its mean and standard deviation. These encapsulate the uncertainty inherent in design values of these parameters. As such, utilizing the mean and standard deviation in lieu of the nominal values of parameters allow for capturing the uncertainties in the probabilistic analysis.

Nominally, the probability of failure is determined by integrating the limit state function over the region where the limit state function is less than or equal to zero as shown in Equation 3.16 (Ayyub and McCuen, 2016).

$$P_f = \int_{Z=-\infty}^{Z\leq 0} f_x(x_1, x_2, \dots, x_n)\, dx_1 dx_2 \dots dx_n \tag{3.16}$$

Where: f_x is the joint PDF of the random vector $\mathbf{X} = \{X_1, X_2, \dots, X_n\}$, and $Z = g(x) < 0$; that is the region of failure. This is further illustrated within the region, $-\infty = Z \leq 0$, where the failure of RC bridge pier due to vehicle impact is expected to occur.

However, determining the probability of failure by evaluating the integral shown above is quite difficult. Alternatively, a reliability index for a structure or structural member can be computed and then used to compute the probability of failure. Converse to the probability of failure, the reliability index (β) is a measure of structural reliability which captures the inherent influence of parameter uncertainties (Der Kiureghian, 2008). Accordingly, several methods have been developed for assessing the reliability of structural members and by extension the probability of failure. These methods fall into three general classes: direct computation via the uncertainty parameters of the limit state equation, Monte Carlo simulations, and moment based methods. These methods usually return slight variations in the reliability index and the probability of failure.

The reliability index is computed using the uncertainty parameters (mean and standard deviation) as shown in Equation 3.17 (Nowak and Collins, 2012).

$$\beta = \frac{\mu}{\sigma} \tag{17}$$

Where: μ is the mean of the limit state equation and σ is the standard deviation of the limit state equation.

However, computing the mean and standard deviation of the limit state equation is sometimes quite impractical especially when the limit state is nonlinear. Also, it presents problems in dealing with limit state equations where the probability distribution is not normal. As a result, an alternate method of computing the reliability index involves using Monte Carlo simulations. This method involves simulating the limit state equation a number of times with changing design variables. These design variables are developed using the uncertainty parameters and randomly generated numbers as shown in Equation 3.18 and Equation 3.19 (Nowak and Collins, 2012).

$$x_i = \mu_x + z_i\sigma_x \tag{18}$$

$$z_i = \Phi^{-1}(u_i) \tag{19}$$

Where: x_i is the computed variable, z_i is standard normal variable, u_i are uniformly distributed random variables between 0 and 1, and Φ^{-1} is the inverse of the standard normal cumulative distribution function.

The limit state equation is then solved using the computed variables. This process is repeated many times using the randomly generated uniformly distributed variables. The probability of failure is then estimated by dividing the number of times the limit state equation falls below 0 by the total number of simulations carried out, and the reliability index can be computed from the probability of failure as shown in Equation 3.20 and Equation 3.21 (Nowak and Collins, 2012).

$$P_f = \frac{n}{N} \tag{20}$$

$$\beta = -\Phi^{-1}(P_f) \tag{21}$$

Where: n is the number of times the limit state was exceeded (g(x) < 0), N is the total number of simulations.

Although generally quite accurate for predicting system reliability, Monte Carlo simulations are computationally expensive, sometimes requiring thousands of simulations to develop accurate estimations of the reliability index. Moment based methods are developed as alternatives to the simulations.

The Hasofer-Lind reliability method is one of these moment based methods. This method is chosen in this study for its advantage over other moment based methods including its invariance to the specific form of the performance (limit state) function unlike FORM and not requiring prior knowledge of the distributions of the variables as required in the Rackwitz Fiessler procedure.

The Hasofer-Lind reliability index is computed using an iterative procedure involving reduced variates, partial derivatives of the limit state function and sensitivity factors as enumerated in Nowak and Collins (2012).

Deriving from the reliability index, the probability of failure is computed as shown in Equation 3.22 (Nowak and Collins, 2012).

$$P_f = \Phi(-\beta) \tag{3.22}$$

Where: Φ(-β) is the cumulative density function of the reliability index.

3.3.5 Sensitivity Analysis

As delineated in the previous section, most parameters involved in analyzing the effect of vehicular impact on concrete piers are random variables subject to variation. An important aspect of studying this effect is understanding the influence of each parameter on the reliability of the structure. Sensitivity analysis allows for a good understanding of this. Used widely in engineering

design and analysis to gain insight into complex model behavior, sensitivity analysis allows for an in depth understanding of the contributions of the uncertainties from individual random variables to the uncertainty of the entire model (Helton et al., 2006; Manring, 2003). The sensitivity of the probability of failure to change in a design variable is computed as shown in Equation 3.23 (Far and Huang, 2019).

$$\frac{\partial P_f}{\partial x} = -\phi(\beta)\frac{\partial \beta}{\partial x} \tag{3.23}$$

Where: x is the design variable, ϕ is the density function of the standard normal distribution and P_f is the probability of failure.

The differential of the reliability index (β) with respect to each design variable can be determined with respect to either the mean of the design variable or its standard deviation as shown in Equation 3.24 and Equation 3.25, respectively (Far and Huang 2019).

$$\frac{\partial \beta}{\partial \mu_x} = \frac{\frac{\partial g}{\partial x}}{\left|\frac{\partial g}{\partial x}\sigma_x\right|} \tag{3.24}$$

$$\frac{\partial \beta}{\partial \sigma_x} = \frac{\frac{\partial g}{\partial x}}{\left|\frac{\partial g}{\partial x}\sigma_x\right|}\frac{x-\mu_x}{\sigma_x} \tag{3.25}$$

Where: g is the limit state equation, μ_x and σ_x are the mean and standard deviations of design variable x respectively.

An explicit examination and derivation of the above equations can be found in Far and Huang (2019).

3.4 Results

3.4.1 Assessment of Reliability

The three described methods are used to estimate the reliability of the concrete pier under vehicular impact. The random variables for the analysis are shown in Table 3-1. The parameters

for the geometric dimensions as well as the material properties are obtained from past studies as published in (Nowak and Collins, 2012). The vehicle mass parameters are obtained from weigh in motion data for the state of Utah (Schultz and Seegmiller, 2006) and the vehicle speed parameters from (Hwang and Nowak, 1991). The stiffness of the vehicle and the pitch of the transverse reinforcement are assumed to remain constant and are not random variables.

Table 3-1 Design Variables and Corresponding Uncertainty Parameters

No.	Variables	Distribution	Mean	CoV	St. Dev.	Units
1	Diameter of pier (d)	Normal	21.06	-	0.25	inches
2	Height of pier (h)	Normal	96.06	-	0.25	inches
3	Vehicle mass (m)	Normal	44663	0.235	18800	lbs
4	Vehicle velocity (v)	Lognormal	110.025	0.165	18.154	ft/s
5	Core diameter (d_c)	Normal	18.06		0.25	inches
6	Yield strength of trans. Reinforcement (φ_s)	Lognormal	45300	0.116	5254.8	psi
7	Compressive strength of concrete (f'_c)	Normal	2760	0.18	496.8	psi
8	Diameter of longitudinal reinforcement (d_l)	Normal	0.855	-	0.365	inches
9	Yield strength of longitudinal reinforcement (φ)	Lognormal	67500	0.098	6615	psi
10	Diameter of transverse reinforcement (d_s)	Normal	0.48	-	0.365	inches
11	Stiffness (k)	Deterministic	1713045	-	-	Lbf/in
12	Pitch (s)	Deterministic	2.5	-	-	inches

Utilizing the three different methods enumerated, the reliability and probability of failure of the pier due to vehicle impact was estimated at different vehicle velocities between 25 mph and 80 mph. Figure 3-3 shows the probabilities of failure at the different speeds for each of the methods.

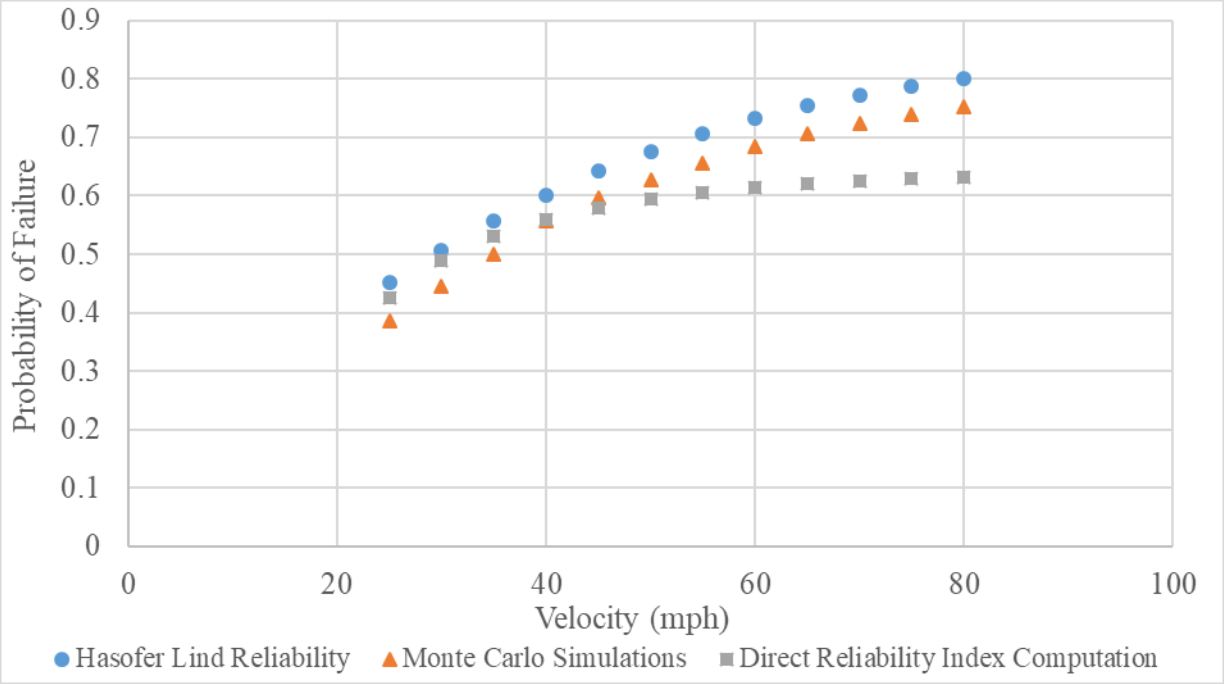

Figure 3-3 Probability of Failure of RC Pier due to vehicle impact at different velocities

From Figure 3-3, it can be observed that the Hasofer-Lind method offers a slightly more conservative estimate of the reliability of the pier compared to the other methods. As a result, the Hasofer-Lind reliability is used for the sensitivity analysis in order to obtain a conservative appraisal of the structural reliability.

3.4.2 Sensitivity Analysis

The sensitivity analysis is carried out to develop an understanding of the effect of each design parameter on the overall uncertainty in the reliability analysis. To test the sensitivity of each parameter, the parameter's design value was changed by a percentage ranging from 0 to 50% of the original design value and the reliability index computed. This was carried out independently for all 10 random variables and the resulting reliability indices plotted are shown in Figure 3-4.

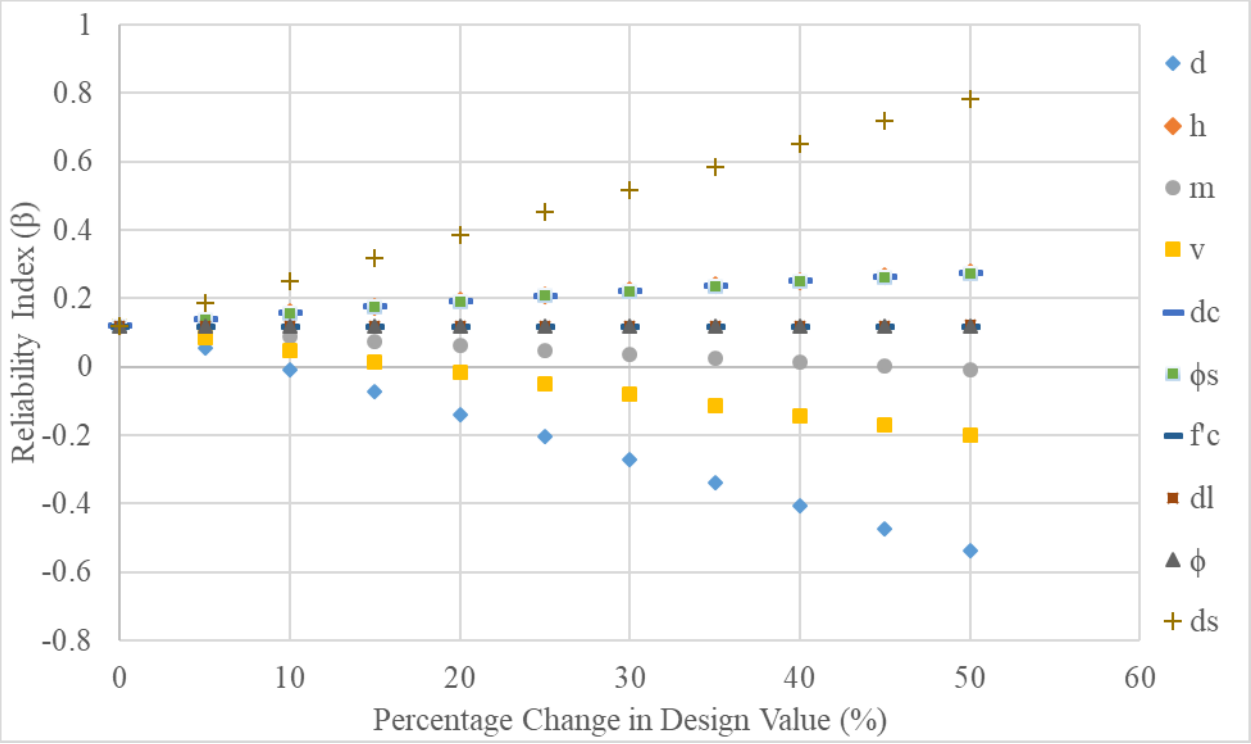

Figure 3-4 Reliability indices for the RC pier at changing design parameters

From Figure 3-4, it can be deduced that the structural reliability of a reinforced concrete pier subjected to vehicular impact is most sensitive to the diameter of the pier and the diameter of transverse reinforcement albeit in diametrically opposite directions. Increasing the diameter of the pier without changing other design parameters will result in a lower reliability index and higher probability of failure for the pier. The opposite is true for changing the transverse reinforcement while keeping other parameters unchanged. Conversely, some design parameters such as the diameter of the main reinforcement and its yield strength have little impact on the response of the pier to vehicle impact.

To quantify the sensitivity of each design parameter to the limit state under consideration, an analysis is carried out as outlined in Equations 3.23 to 3.25 (Far and Huang, 2019). Table 3-2 shows the results of this analysis.

Table 3-2 Sensitivity of Each Design Parameter to the Limit State

No.	Variable Name	$\partial\beta/\partial\mu$	$\partial P_f/\partial\mu$	$\partial\beta/\partial\sigma$	$\partial P_f/\partial\sigma$
1	Diameter of pier	-0.0670	0.0262	-0.0002	8.8465E-05
2	Height of pier	0.0049	-0.0019	-1.2243E-06	4.7860E-07
3	Vehicle mass	-7.9289E-06	3.0997E-06	-3.6619E-07	1.4316E-07
4	Vehicle velocity	-0.0219	0.0085	-0.0006	0.0002
5	Core diameter of pier	0.0259	-0.0101	-3.3794E-05	1.3211E-05
6	Yield strength of trans. reinforcement	1.0329E-05	-4.0378E-06	-1.1290E-07	4.4137E-08
7	Compressive strength of concrete	1.0251E-06	-4.0076E-07	-1.0515E-10	4.1105E-11
8	Diameter of longitudinal reinforcement	0.0028	-0.0011	-5.9100E-07	2.3104E-07
9	Yield strength of longitudinal reinforcement	9.640E-10	-3.7686E-10	-1.2380E-15	4.8398E-16
10	Diameter of transverse reinforcement	2.6373	-1.0310	-0.5113	0.1999

Table 3-2 gives the sensitivity derivatives for each design parameter involved in the vehicle impact limit state. These derivatives quantify the observations made from the plots in Figure 3-4. The signs of the derivatives tell us the relationship between the design parameter and the limit state equation. The value of the derivative on the other hand tells us the relative strength of this relationship. For instance, if the sensitivity derivative is large, then small changes in the value of its corresponding random variable will have a large impact on the resulting reliability of the structural member and vice versa.

From the values, it can be deduced that the diameter of transverse reinforcement has the greatest positive correlation with the reliability and the diameter of the pier has the greatest negative correlation. Consequently, these parameters will have the greatest influence on the reliability of the pier under vehicular impact. The yield strengths of both longitudinal and transverse reinforcements have very little effect on the reliability index as established by their very small sensitivity derivatives. Also, the velocity of the impacting vehicle is a much more critical

factor in the reliability of the pier than the mass of the vehicle although both variables have a negative correlation with the reliability index.

It should also be kept in mind that although the analysis assumed independence of the variables, in design there are some interdependencies within them. For instance, the diameter of the core is dependent on the diameter of the pier. Another important relationship is the reinforcement ratio in order to control cracks followed by the failure in tension (ACI, 2011).

From the sensitivity analysis, it is determined that although the performance of the pier depended on both the outside and core diameters, these variables had very contrasting effects on the performance. Increasing the core diameter results in increased performance and vice versa while the opposite was the case with the outside diameter. However, in designing structural members, these two parameters cannot operate in isolation. Figure 3-5 shows the sensitivity performance of the pier while changing both parameters in tandem.

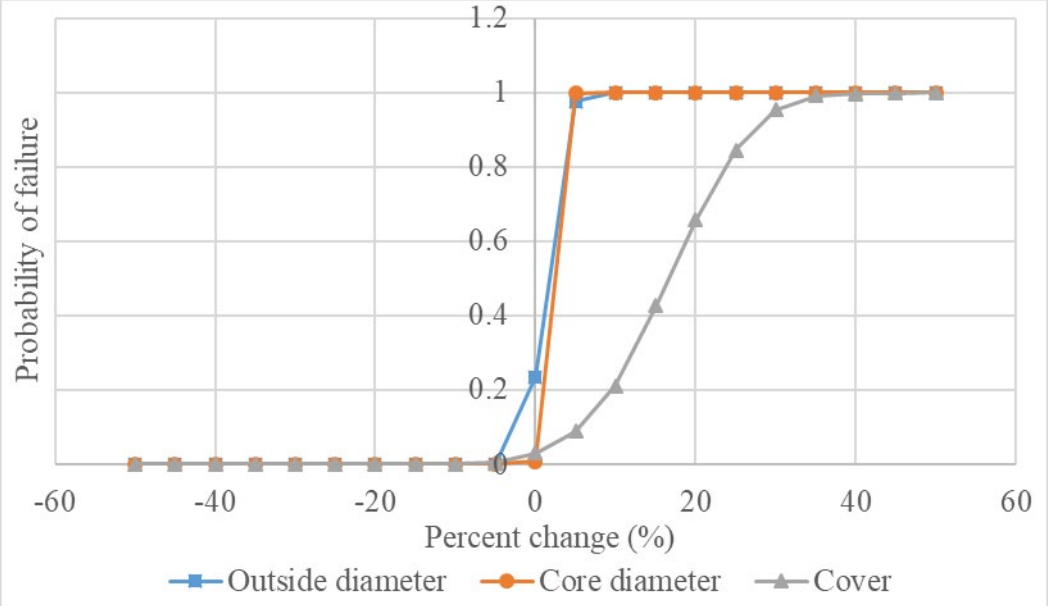

Figure 3-5 Sensitivity of RC pier to External and Core Diameters

From the plot, it can be deduced that changing both the outside diameter and the core diameter while keeping the cover consistent results in quite similar patterns of performance for the pier

irrespective of which is changed. However, changing the cover size could result in an enhanced performance of the pier. As such, it might be more beneficial to change the cover size to improve the pier's performance in impact scenarios rather than a change in the diameter.

The reliability analysis shows an insight into the expected performance of the RC bridge pier undergoing vehicular impact. By contrast, a deterministic analysis of the pier under a similar scenario will not account for the uncertainties in the parameters and as such may critically underestimate the behavior. For instance, a deterministic analysis using the nominal design values results in a dynamic impact force of about 39 kips and a dynamic shear capacity of approximately 110 kips, essentially assuring of no failure of the pier under the specific loading scenario. A probabilistic analysis however, indicated a probability of failure of 0.45 indicating 45 percent possibility of exceeding the capacity. This is quite a high risk of exceedance which could not be captured in the deterministic analysis.

3.5 Conclusions

In this research, statistical data for random variables is utilized to assess the probability of failure for a vehicle impacted RC bridge pier, in order to define the performance of the bridge pier under this loading scenario. This analysis is useful for understanding both the reliability of in-service bridge piers and their vulnerabilities to vehicle impact scenarios.

In order to determine the failure, a limit state model is defined, incorporating damage indices of the defaced RC bridge pier. Design parameters for the RC bridge pier are used as random variables in the reliability analysis. The structural reliability was evaluated using three different methods. The Hasofer-Lind reliability method was determined to be the most conservative and used for the subsequent sensitivity analysis. Results from reliability analysis indicate probabilities of failure of the pier ranging from 45% to 80% for a vehicle at different

velocities from 25 mph to 80 mph. Sensitivity analyses are undertaken to understand the relationship between the individual design variables and the corresponding reliability. Results show that increasing the diameter of the pier without changing other design parameters will result in a lower reliability index and higher probability of failure for the pier. The opposite is true for changing the transverse reinforcement while keeping other parameters unchanged. The underlying relationship between the external and core diameters was also explored to understand how the relationship between these variables affect the system reliability.

In conclusion, the reliability analysis has shown that impact loads have to be an important consideration in designing bridge piers as they have quite a sizable effect on the performance. This importance may not be captured by deterministic analysis as it does not capture the uncertainty in the design variables.

CHAPTER 4 Residual Capacity of Vehicle Impacted RC Bridge Pier

4.1 Introduction

The increasingly widespread incidences of vehicles colliding with bridge piers has had a significant impact on the integrity of existing bridge structures. Degradation of the capacity of the support structure from the impact leads to an overall deterioration of the structure and could result in catastrophic failures including total collapse. Some collision accidents result in severe damage to bridge structures, such as pier fracture and bridge collapse, while others cause localized damage limited to the impact location such as concrete cracking. Reinforced concrete (RC) piers are commonly used as vertical piers. During their service lives, piers may suffer damage from impact forces occurring due to vehicle collisions, which varies according to vehicle density and usage. A statistical investigation (Sharma et al., 2014) showed that about 210 bridge failures are triggered by vehicle collisions over the nine-year period covered by the investigation (1996-2005). Piers are found to be more vulnerable to vehicle collisions than to other hazardous loads such as earthquake and blast, resulting in serious damage and casualties. To understand the behavior and accurately analyze bridge failure patterns and failure modes of the damaged piers, it is necessary to study and investigate these structures in depth. As such, many studies have been devoted to understanding the response of RC piers subjected to vehicle impact. To limit the consequences of such events and improve the overall structural integrity of bridges, the development of analytical techniques tailored towards capturing the effects of vehicle impact damage on bridge structures is very important. Analytical techniques used in the analysis and design of piers can be tailored for this purpose.

Some vehicle-pier collisions have resulted in severe damage such as pier fracture, bridge-pier dislocation, and bridge collapse. Other collisions, which only cause slight damage to the

piers, such as concrete cracking at the impact location, could also have long-term implications for the integrity of the bridge. To comprehensively assess the behavior and failure modes of the damaged piers, it is necessary to accurately analyze the peak impact force, the maximum deformation, impact force, impact duration, and deformation time histories of the piers. These indices are also helpful in designing protection schemes for piers to prevent vehicle collision.

Improved understanding of the effects of the deterioration from vehicle impact on the structural performance of reinforced concrete piers will enhance current inspection procedures, and can be used in planning strategic and cost-effective rehabilitation methods. Therefore, the objective of this research is to develop an analytical bridge pier strength evaluation method that can be incorporated into currently used bridge condition evaluation methods. In addition, an attempt is made to establish a rating system to categorize damaged piers according to the severity of damage. This rating system utilizes the results from the evaluation process to categorize the piers as either needing re-strengthening in which case, they can be retrofitted and their service lives increased, or seriously damaged and needing replacement. The final proposed evaluation method provides accurate information on the condition and load-carrying capacity of bridge piers after damaging impact events.

An existing approach for evaluating post-earthquake damage and residual performance of piers developed using a nonlinear model updating approach and tested on ultra-high performance steel fiber reinforced concrete (UHPSFRC) is primarily focused on the effects of seismic loads on the bridge piers and does not consider other impact loads and their effects (He et al., 2019). A damage criterion developed for reinforced concrete piers based on the residual axial load carrying capacity proposed using a numerical approach to develop pressure-impulse diagrams to indicate the intensity of damage from impact resulting from blast loads on the pier (Shi et al.,

2008; Thomas et al., 2018). Other studies utilizing finite element modelling to assess post blast damage behavior of bridge piers have shown the potential of developing the ability to accurately determine the damage and subsequent loss of capacity of a reinforced concrete pier after impact events (Bao and Li, 2010; Zhou and Li, 2018). In addition, the performance of bridge piers after vehicle impact events has been also studied (Abdelkarim and El Gawady, 2017). However, a holistic numerical approach to investigating post impact damage as well as residual capacity of the defaced piers for serviceability limit states is yet to be developed. This chapter proposes an innovative approach using the dynamic impact factor (DIF) for both concrete and reinforcing steel as well as a model extrapolated from prior experimental and simulated studies to predict the residual capacity of bridge piers damaged from vehicle impact in a practical manner.

4.2 Materials

In order to analyze the serviceability, strength and behavior of the circular reinforced concrete bridge pier during and immediately after vehicular impact, a representative test pier specimen is utilized. The specifications for the test pier are obtained from the Utah Department of Transportation (UDOT), as per Report No. UT-14.09 (Pantelides et al., 2014). Constructed using a concrete grade of 3 ksi (20.7 MPa), the pier has longitudinal reinforcement (primary reinforcement) of six #8 steel (grade 36 ksi) re-bars throughout its entire length including the foundation with a spirally arranged shear reinforcement of #4 steel (grade 36 ksi) rebar at 2.5 inches (63.5 mm) pitch throughout. The height of the test pier is taken as 8 ft.6 in. (2.591 meters), with varying cross-sections; octagonal from the foundation level up to a height of 7 ft. (2.134 meters) and rectangular the rest of the way up. The gross cross-sectional area of the pier has been estimated using the weighted average method as recommended by ACI 318R-05 (ACI, 1985). For simplification purposes, a circular cross section was assumed, and its

dimensions selected to match the cross-sectional area of the representative pier. Details of the pier cross-section are shown in Figure 4-1.

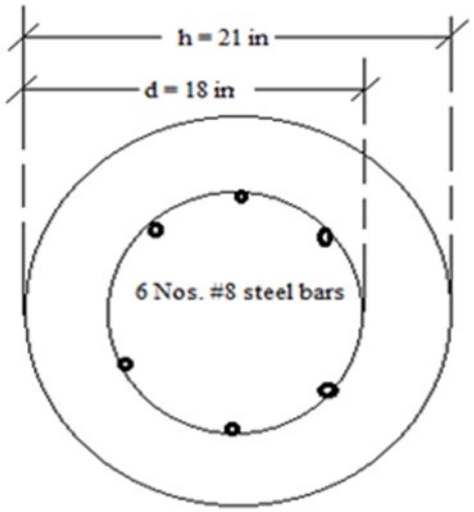

Figure 4-1 Pier Cross Section

For the impact loading, a vehicle moving at high speed is assumed as per previous studies (Abdelkarim and El Gawady, 2017). When a high-speed vehicle hits the reinforced concrete (RC) bridge pier, the impact effect is amplified due to the high steel strain rate, and substantial impulse is produced due to the dissipation of kinetic energy caused by the considerably high vehicular momentum.

4.3 Methodology

4.3.1 Frontal Impact of Bridge Pier

When an exposed reinforced concrete bridge pier experiences vehicular impact, there is a possibility of substantial damage to that pier and by extension, the bridge. In some cases, the damage is so extensive that the bridge completely collapses. Right after impact, the high frontal shock from the impact causes an overpressure (impulse) that actually damages the bridge piers, frequently to the point of collapse. In some cases, the bridge piers suffer relatively less damage

and therefore can be revamped and returned to service. Figure 4-2 shows a representative time history of a vehicular impact event.

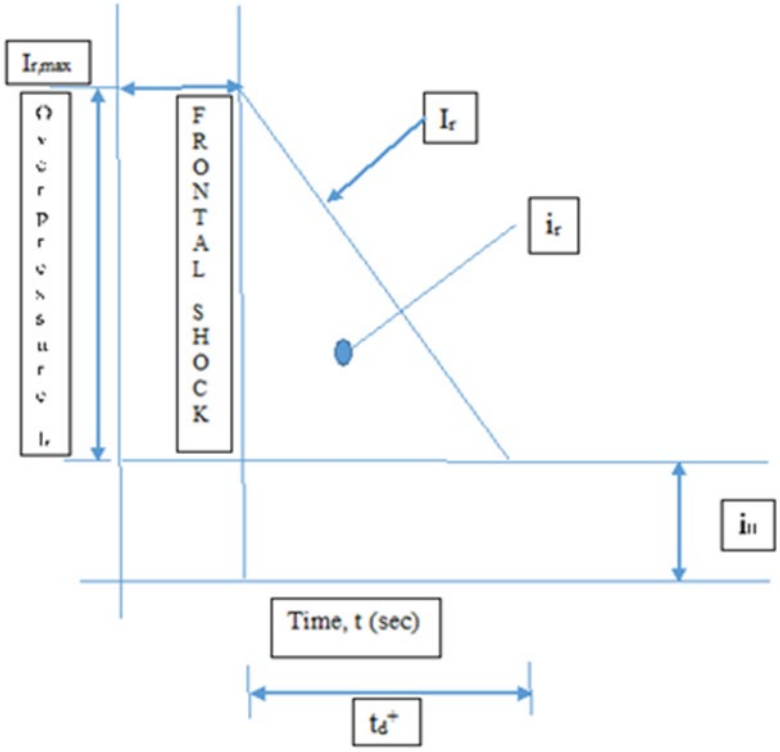

Figure 4-2 Impact Pressure Diagram on the RC Bridge Pier

The time dependent frontal shock from vehicular impact can be computed using an averaged integration of the instantaneous impact force over the range of 50 ms neat the peak impact force as shown in Equation 4.1 (Zhou and Li, 2018):

$$I_{dyn} = \frac{\int_{t_d-0.025}^{t_d+0.025} I_r \sin\left(\frac{\pi t_d^+}{t}\right) di}{0.05} \tag{4.1}$$

Where: I_{dyn} represents the frontal shock due to impact, $I_{r,}$ is the peak reflected pressure (overpressure), t_d^+ is the time instant of the peak impact force, and t represents the impact duration.

The relationship shown in Equation 4.1 can be used to estimate the total static force from the instantaneous peak force occurring during vehicular impact, capturing the expected loading history of the vehicle impact over time on the RC pier. This equation utilizes the expected sinusoidal loading pattern of the vehicular impact event to extrapolate the dynamic load from the peak force and the loading time history.

The overpressure represented by $I_{r,}$, is a function of the kinetic energy from the impacting vehicle and can be determined using Equation 4.2, developed as a relationship between bending stress developed in the pier from the peak dynamic force of impact and kinetic energy using data from various simulated and experimental studies (Cao et al., 2019; Gomez and Alipour, 2014; Mohammed and Parvin, 2013; Zhou and Li, 2018). The bending stress was used in lieu of the impact force so as to capture the possible effects of geometric variations of the pier in the resulting overpressure at impact.

$$I_r = (4 * 10^{-5} E) * \frac{4I}{(L*c)} \tag{4.2}$$

Where: E is the kinetic energy, absorbed by the impacted pier, I is the moment of inertia of the pier, L is the height of the pier and c is the perpendicular distance from the neutral axis of the cross section to the farthest point on the cross section of the pier.

Assuming the vehicle comes to rest without rebounding from the pier, the kinetic energy (E) equation is determined as the kinetic energy of the vehicle using Equation 4.3 (Tsang and Lam, 2008).

$$E = 0.5 M_{veh} V^2 \tag{4.3}$$

Where: M_{veh} represents the mass of the impacting vehicle, E is impact energy of the vehicle, and V is the frontal impact velocity of the vehicle causing instability of the pier.

4.3.2 Determination of Damage Index

The damage to the reinforced concrete material from the impact load can be described using a damage index (λ). The damage index plays a significant role in characterizing the severity of damage to the structure. This index, λ, can be determined using the expression in Equation 4.4.

$$\lambda = I_{dyn}/V_{dyn} \tag{4.4}$$

Where: 'I_{dyn}' is the vehicle dynamic impact force and V_{dyn} is the dynamic shear.

Furthermore, the dynamic shear, V_{dyn}, and shear capacity of the pier, V_n, are related by the relationship in Equation 4.5 (Feyerabend, 1988).

$$V_{dyn} = V_n \cdot (DIF) \tag{4.5}$$

Where: DIF is the dynamic impact factor, and V_n is the shear capacity of the reinforced concrete pier with spiral transverse shear reinforcement.

The dynamic impact factor (DIF) can be expressed in terms of quasi-static strain rate (έ) and is expressed as shown in Equations 4.6 to 4.8 (Mander et al., 1988).

$$DIF = \left(\frac{\acute{\varepsilon}}{10^{-4}}\right)^{\xi} \tag{4.6}$$

$$\xi = 0.019 - 0.009(\sigma_{dyn}/60) \tag{4.7}$$

$$\sigma_{dyn} = [1 + (\acute{\varepsilon}/C)^{1/P}] \cdot (\sigma_p + \beta E_p \varepsilon^{eff}) \tag{4.8}$$

Where: έ is the strain rate, ξ is a constant which depends on the dynamic yield stress of steel at the strain hardening zone, σ_{dyn} is the dynamic yield stress of steel, σ_o is the initial yield stress, which is taken as 60 ksi (420 MPa) as per ASTM A706 for the yield stress at the elastic zone for grade 60 steel rebar, ε^{eff} is the equivalent plastic strain, taken as 0.72, E_p is the plastic hardening modulus, β is the hardening parameter, which ranges from 0 to 1 and is taken as 0.5 in this study, έ is the quasi-static strain rate, which is taken as 5.4 x 10^{-4} s^{-1} (Feyerabend, 1988), and parameters C and P are constants.

The modulus of elasticity of the steel rebar at the strain hardening stage, E_P, is determined using Equation 4.9.

$$E_p = \sigma_P / \varepsilon_{eff} \tag{4.9}$$

The yield stress, σ_P, at the plastic region used in this equation is 8.612 ksi (59.376 MPa) and the plastic strain, ε_{eff}, used is 0.72 (ACI, 1985). The modulus of elasticity, E_P, is determined to be 11.94 ksi (82.32 MPa) (Mander et al., 1988). Inserting these values into Equation 4.8, results in a dynamic yield stress (σ_{dyn}) of 68.61 ksi (473.05 MPa).

Using Equation 4.7 with the dynamic yield stress σ_{dyn} at 68.61 ksi (473.05 MPa) yields ξ as 0.0175, resulting in a DIF (dynamic impact factor) of 1.07 using Equation 4.6.

Using the DIF value obtained, the dynamic shear force (V_{dyn}) can be determined for the said pier using Equation 4.5. The dynamic shear force (V_{dyn}) is thus a function of vehicular mass, impact velocity, and impact duration. As such, it can be opined that these variables play a significant role in detecting the damage pattern of the damaged pier.

4.3.3 Computation of the Residual Strength of Damaged Pier

The residual capacity of the damaged pier can be determined using the damage index (λ), computed as shown in Equation 4.4. The severity of damage is scaled according to the damage index, λ, as follows: λ = 0-0.2 is low damage, 0.2-0.5 is medium damage, 0.5-0.8 is high damage, and 0.8-1 is collapsed and no longer in service (Shi et al., 2008). For both the highly damaged and the collapsed case, the structural members require immediate replacement.

Depending on the severity of the damage to the pier, the pier could be retrofitted and returned into service if only minimally damaged, or totally replaced if the severity ranges from highly damaged to complete collapse. The relationship between the damage index and residual strength of the damaged pier is shown in Equation 4.10 (Shi et al., 2008).

$$\lambda = 1 - \left(P_{N,residual}/P_{N,design}\right) \tag{4.10}$$

Where: $P_{N,\,residual}$ is the residual strength of the damaged pier after vehicular impact and $P_{N,\,design}$ is the design axial load carrying capacity of the undamaged reinforced concrete bridge pier as stated in ACI.

Rearranging Equation 4.10 allows for the determination of the residual strength of the damaged RC pier as shown in Equation 4.11 (ACI, 1985; ASCE, 2013).

$$P_{N,residual} = (1 - \lambda) \cdot P_{N,design} \tag{4.11}$$

The design axial capacity, $P_{N,\,design}$ can be computed using Equation 4.12, as per ASCE (2013).

$$P_{N,design} = 0.85 f_c'\left(A_g - A_s\right) + \sigma_0 \cdot A_s \tag{4.12}$$

Where: f_c' is the 28-day compressive strength of concrete, σ_o is the yield strength of steel, and A_g and A_s are the gross cross-sectional area of concrete and total cross-sectional area of longitudinal steel, respectively.

As suggested in ASCE and ACI 426 the design shear capacity of the reinforced concrete pier is determined using Equation 4.13 (ACI, 1985; ASCE, 2013).

$$V_{N,design} = V_c + V_s \tag{4.13}$$

Where: V_c is the shear strength carried by the concrete and V_s is the transverse shear capacity.

The shear strength, V_c, is computed as shown in Equation 4.14 (ASCE, 2013).

$$V_c = \nu_b[1 + 3P_{N,design}/f_c' \cdot A_g] \cdot A_e \tag{4.14}$$

Where: A_g represents the gross cross-sectional area of the concrete in the pier and A_e is 80% of A_g, i.e. A_e becomes $0.8A_g$, and ν_b is the shear constant.

The shear constant (ν_b) is determined using Equation 4.15 (ASCE, 2013).

$$\nu_b = [0.0096 + 1.45\rho_t] \cdot (f_c')^{1/2} \leq 0.03(f_c')^{1/2} ksi \tag{4.15}$$

Where: ρ_t is the longitudinal steel ratio and $P_{n,\ design}$ represents the axial load capacity of the reinforced concrete pier.

Furthermore, the transversal shear capacity, V_s is calculated using Equation 4.16 (ASCE, 2013).

$$V_s = \pi/2\, A_h \sigma_{yh}\, D'/s \tag{4.16}$$

Where: A_h is the area of a single hoop or spiral, $D^{'}$ is the spiral or hoop diameter, s denotes the pitch of the helix, and σ_{yh} represents the yield stress of transverse steel.

Using Equation 4.11 and replacing $P_{N,\ design}$ with $V_{N,\ design}$, the residual shear capacity of the reinforced concrete pier can also be determined.

4.4 Results

4.4.1 Analysis Parameters

The gross cross-sectional area of the test pier is 346.5 in^2 (0.224 m^2). The design axial load carrying capacity of pier, determined using Equation 12 as recommended in ACI 318R-05 (ACI, 1985) is 1150 kips (521.63 tons). In this study, both ideal axial compression and shear capacity are assumed.

4.4.2 Residual Capacity of Pier after Impact

Several vehicle masses are used in calculating the residual capacity of the reinforced concrete pier. These respective masses of 80,000 lbs., 74,000 lbs., 34,000 lbs., and 26,000 lbs. respectively, (40 tons, 37 tons, 17 tons and 13 tons) are utilized in determining the relationship between the vehicular mass and the extent of damage incurred by the pier as represented by the residual capacity. Figure 4-3 shows the relationship between the vehicle speed and the dynamic impact force for the different vehicle masses simulated. These masses, exhibit similar correlations between the speed and impact force, with a steady increase in the expected dynamic

impact force at increasing speeds. This relationship is more clearly defined with increasing masses of the vehicles resulting in a steeper increase in the dynamic impact force at increasing speeds. Furthermore, this indicates that the vehicle speeds are of heightened importance in impact scenarios with increasing vehicle masses. The diminishing trend of the residual capacities of the impacted bridge pier has similar characteristics both for axial and shear.

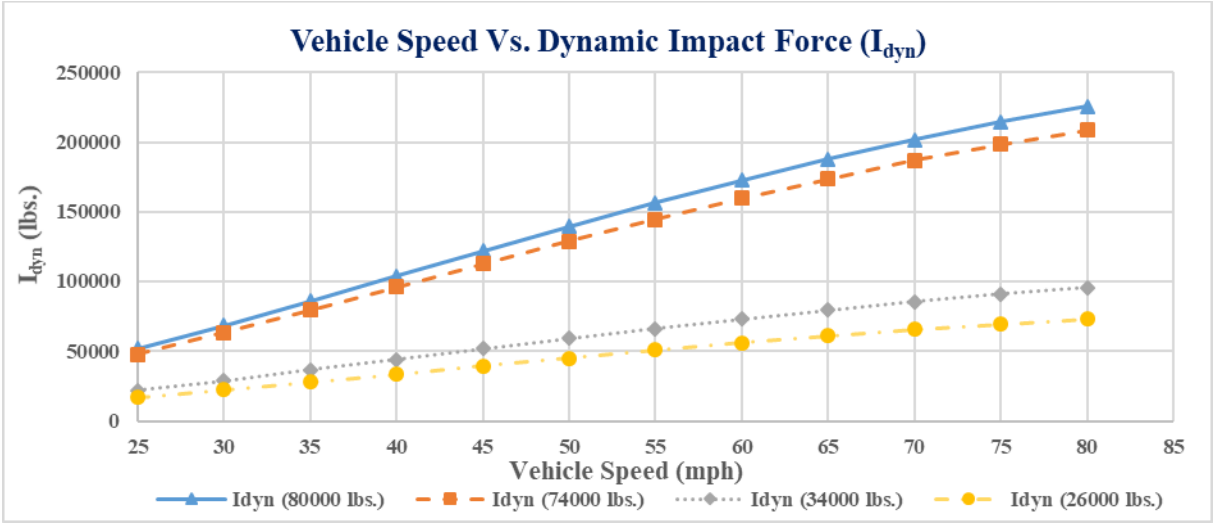

Figure 4-3 Relationship between Dynamic Impact and Vehicle Speed for Different Vehicle Masses

As to be expected from the linear relationship between the dynamic impact force and vehicle speed, there is an inverse relationship between the residual capacity of piers and vehicle speeds with the post impact residual capacity decreasing at increasing impact velocities. As shown in Figures 4-4 and 4-5 for the axial and shear capacities respectively, this relationship is increasingly evident with an increase in the mass of the impacting vehicle, with relatively little change for smaller vehicles and a steep drop in the residual capacity across different speeds for the larger vehicles.

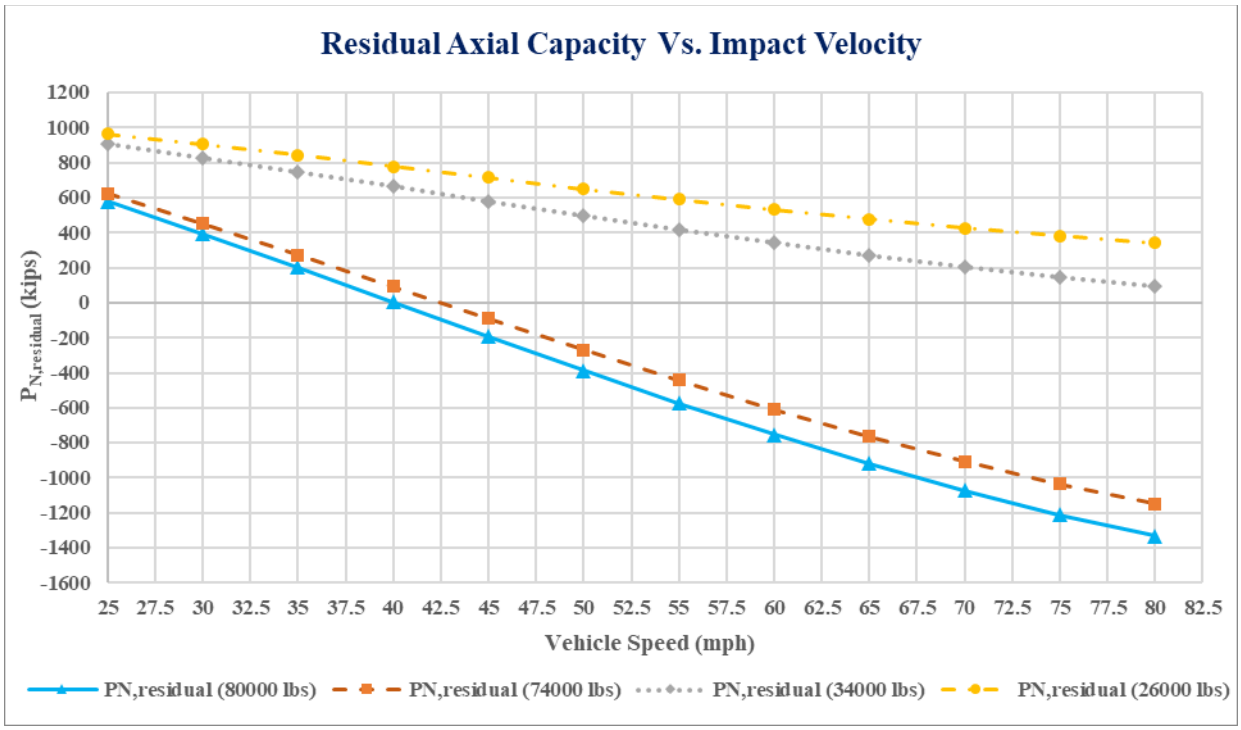

Figure 4-4 Residual Pier Axial Capacity at Different Vehicle Speeds

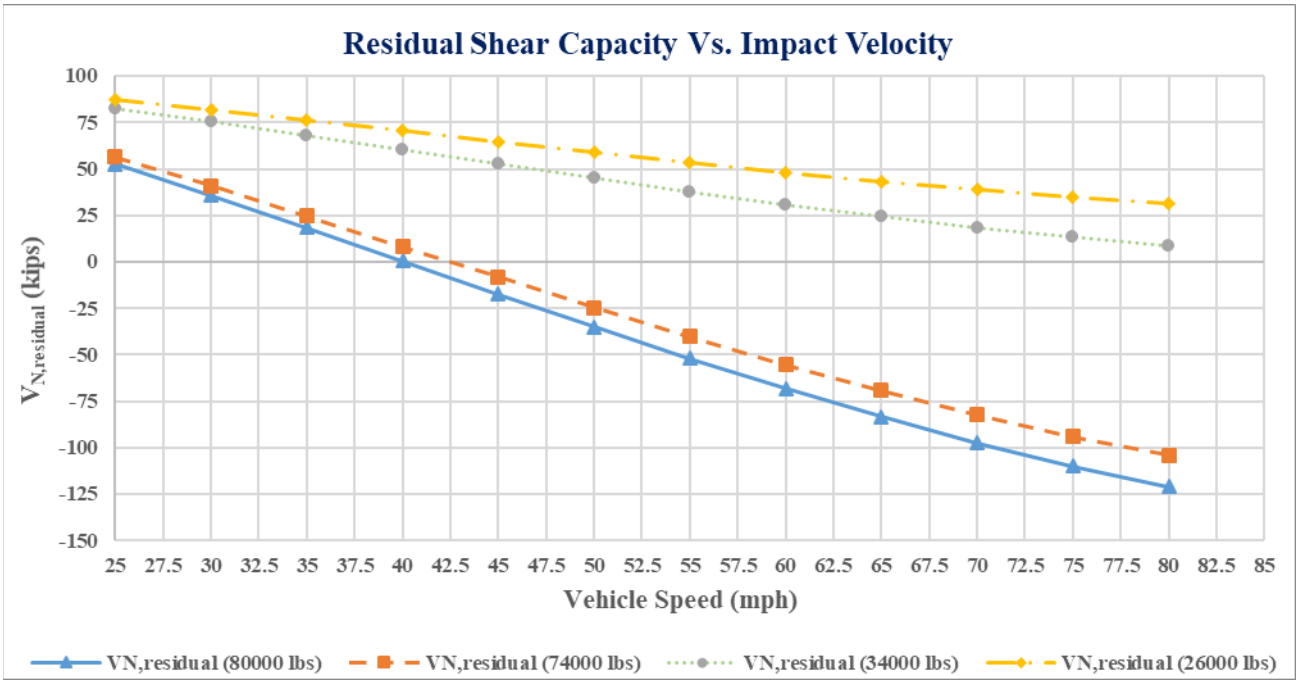

Figure 4-5 Residual Pier Shear Capacity at Different Vehicle Speeds

From these figures, it can be observed that at even relatively low speeds of 40 mph (64 k/hr.) vehicles with higher masses (74000 and 80000 lbs.) can have a devastating effect on reinforced

concrete piers, leaving them with no residual capacity whereas lower masses (34000 and 26000 lbs.) will have a less deleterious effect, leaving the pier with substantial residual capacity allowing for possible repairs and retrofitting for continued service. These results obtained via simulations from a model extrapolated from data obtained from various sources agree with the intuitive conjecture that increased vehicle masses will cause more damage to piers on impact. As such, this model could viably be used for the extrapolation of the residual capacity of piers of varying geometric dimensions after impact by vehicles with diverse variables of mass and velocity.

4.4.3 Relationship between Pier Parameters and Residual Capacity

Figures 4.6 and 4.7 show the relationships between the vehicular momentum and residual capacity of the pier in axial and shear respectively. From the plots, it can be deduced that there is an inverse relationship between the residual capacity of the pier and the vehicular momentum with the capacity reducing with a corresponding increase in the vehicular momentum at impact. However, the extent of this relationship seems to be dependent particularly on mass as there is a slight divergence in the change in capacity with momentum of the smaller vehicles. This implies that the mass of the vehicle has a predominant effect on vehicular impact scenarios.

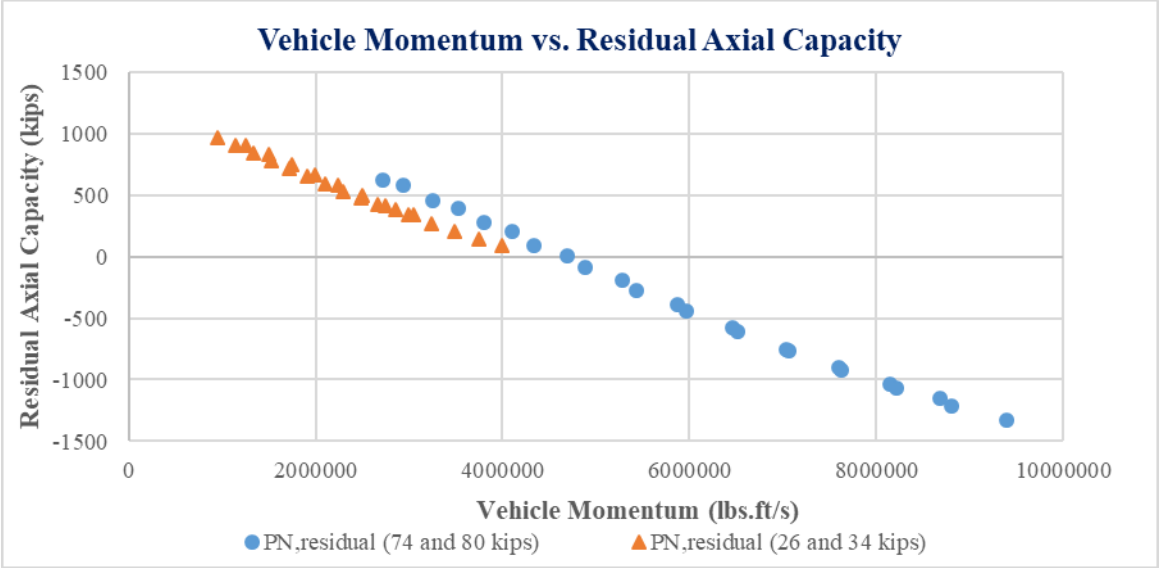

Figure 4-6 Vehicular Momentum and Residual Axial Capacity of Pier

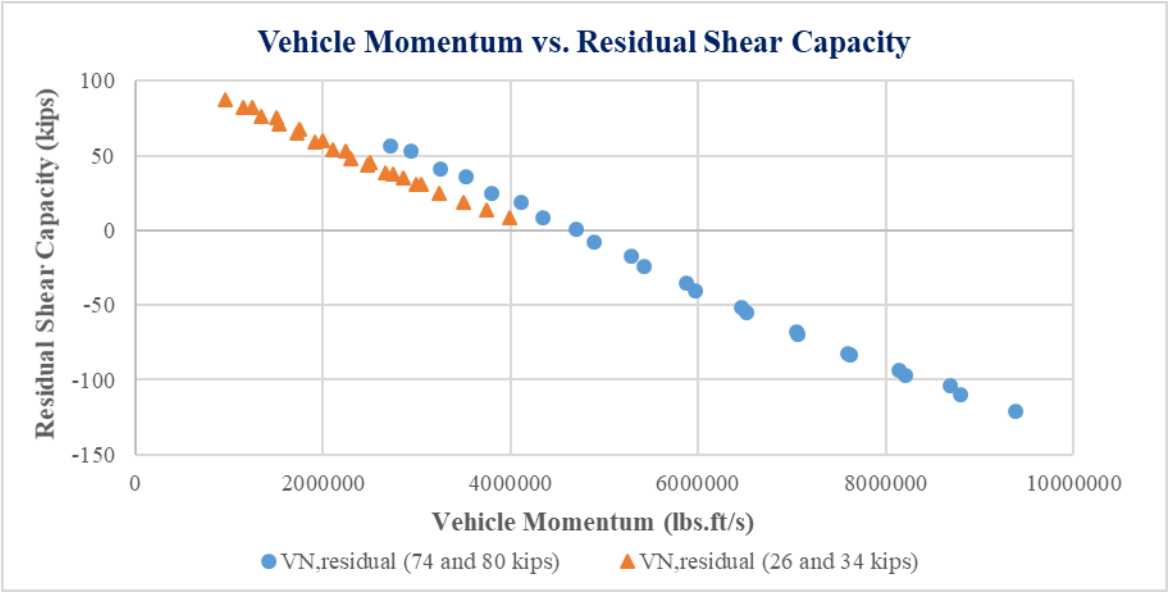

Figure 4-7 Vehicular Momentum and Residual Shear Capacity of Pier

Figure 4-8 shows the relationships between the dynamic impact or peak frontal shock exerted by a vehicle on the pier to the residual to design pier load ratio. From the figures, it can be inferred that as the dynamic impact increases, there is a linear decrease in the pier axial load ratio. For the

pier to retain 50% or more of its axial capacity, the dynamic impact of the vehicle needs to be limited to approximately 50 kips (222.4 kN).

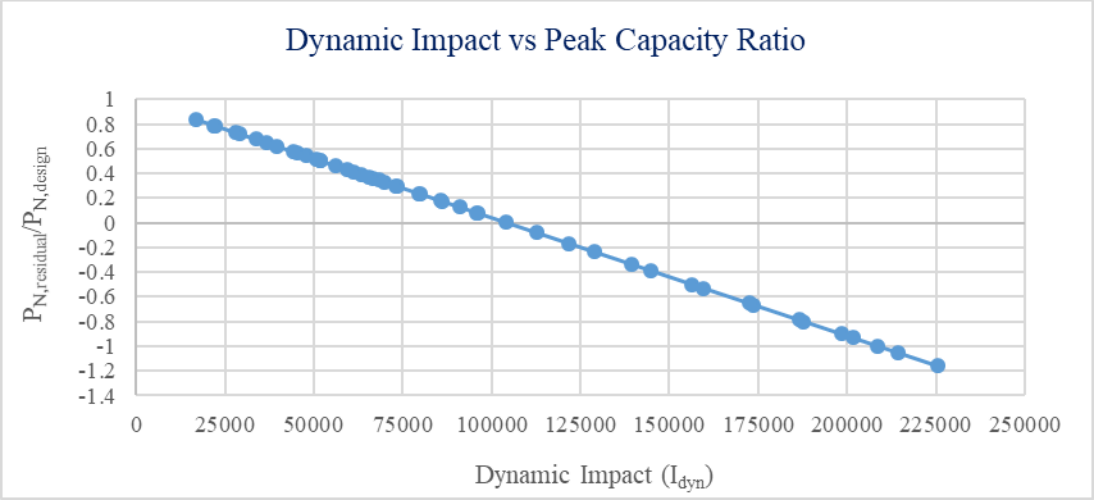

Figure 4-8 Relationship between Dynamic Impact and Pier Load Ratios

The relationships between the damage indices (λ) and the ratios of the residual pier axial capacity and its design capacity is shown in Figure 4-9. From the figure, there is a steady drop in axial residual capacity with increasing damage indices.

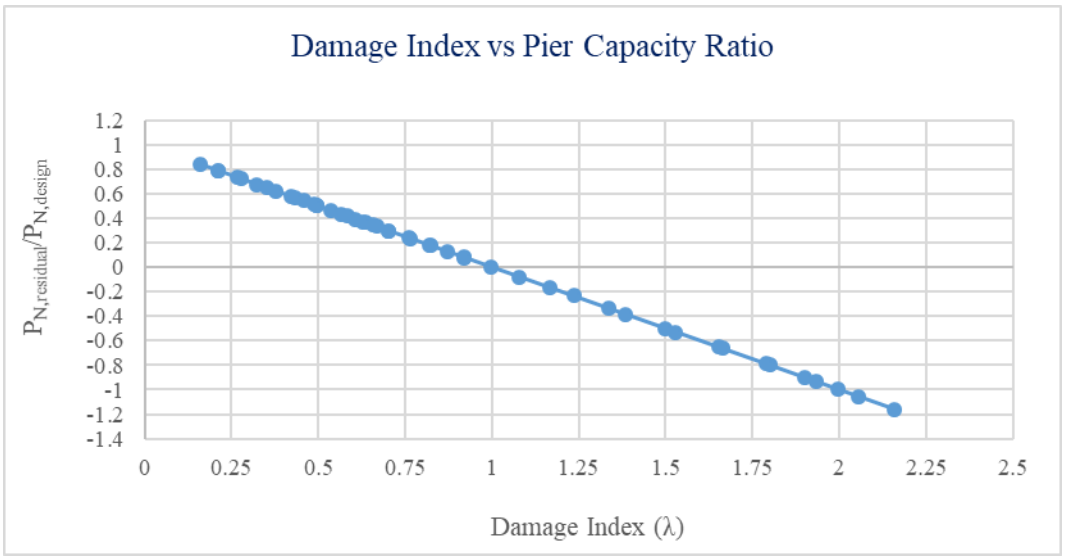

Figure 4-9 Damage Indices with the Pier Capacity Ratio

There is a strong negative correlation between the pitch and the residual capacity of the pier in axial and shear. As shown in Figures 4-10 and 4-11, for an impact velocity of 70mph (112.65 km/hr.), there is a decrease in shear with the pitch increasing from 2 to 5.5 inches. This can be attributed to the direct relationship between the reinforcement pitch and design shear capacity. Increasing the pitch of the reinforcement results in a direct decrease in the design shear capacity and by extension an increase in the damage index. This in turn leads to a decrease in the expected post impact capacity of the pier.

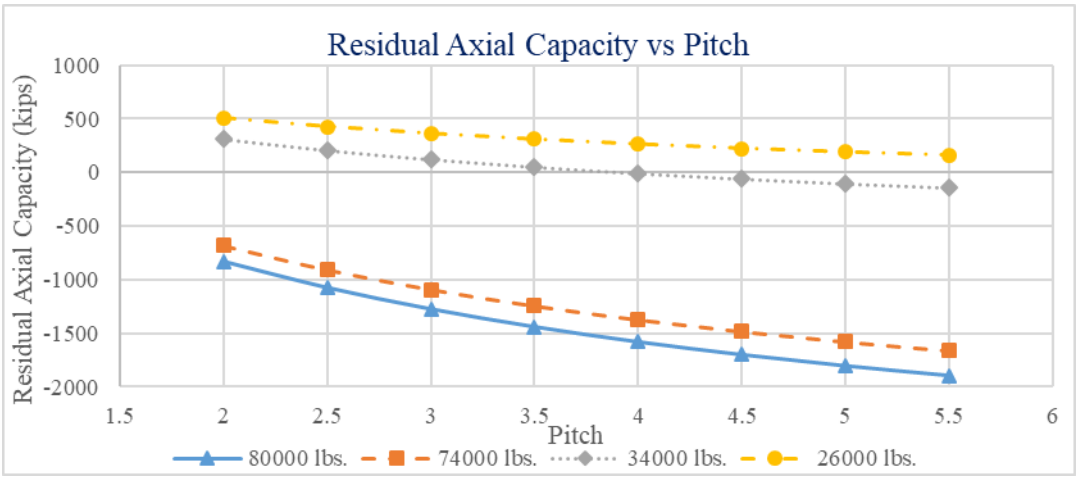

Figure 4-10 Relationship between Shear Reinforcement Pitch and Residual Axial Capacity

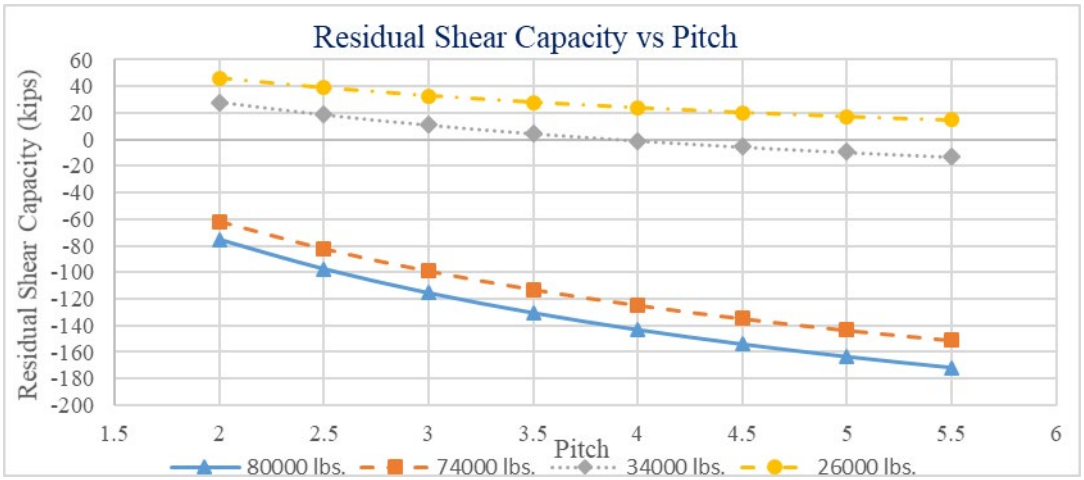

Figure 4-11 Relationship between Shear Reinforcement Pitch and Residual Shear Capacity

These results of preliminary studies into the development of a performance-based damage assessment methodology for reinforced concrete (RC) bridge piers subjected to vehicular impact provide a number of insights. During impact from a vehicle, RC piers sustain different levels of damage depending on the geometry, material properties, and boundary conditions of the pier as well as the mass, velocity, and type of vehicle. Damage incurred by the pier also depend on the impact duration and the maximum dynamic impact shock (I_{dyn}) transmitted into the RC pier. The severity of damage to the pier is dependent on these factors and influences the decisions to be made regarding further use of the pier. Some piers sustain little damage and can be retrofitted and strengthened for continued service, while others which suffer more extensive damage will require immediate replacement should the bridge need to be kept in service.

The severity of damage from vehicle impact on RC bridge piers is categorized into four levels each of increasing severity. These categories, which are defined using damage indices (λ), are in increasing order of severity: low, medium, high damage and total collapse. From previous studies, piers having damage indices from 0.1 to 0.3 classified as low damage can be retrofitted and restored to service, whereas those with damage indices ranging from 0.4 to 0.6 classified as medium damage need special attention during retrofit. High damage and total collapse corresponding to damage indices 0.6 to 0.8 and 0.8 to 1.0 respectively, require immediate replacement. In this study, an attempt is made to quantify the damage using the vehicle impacted dynamic shear (V_{dyn}) and beyond that utilize the computed damage index to determine the residual strength of the pier both in terms of axial and shear capacity with respect to the peculiarities of the impact scenario. A model relating the geometric dimensions of the pier and the peak impact force at impact t the kinetic energy of the impacting vehicle was developed for this purpose. The defined

process can be used to deduce the expected behavior of a reinforced concrete pier during and after the occurrence of an impact scenario.

A relationship between the damage indices previously developed to characterize the damage to the piers (Shi et al., 2008), and the residual capacity of the damaged pier has also been established. This relationship as shown in Table 4-1 indicates that there is a negative correlation between the damage index and the axial residual capacity of the pier with a steady increase in residual capacity at decreasing damage indices.

Table 4-1 Damage Index Level Compared to Residual Pier Capacity

Damage Indices (λ)	**Residual Pier capacity, $P_{N, residual}$ (kips)**
0	1150
0.2	920
0.5	575
0.8	230
1.0	0

This negative linear relationship between the residual pier capacity of the impacted pier and the corresponding damage indices is further illustrated in Figure 4-12.

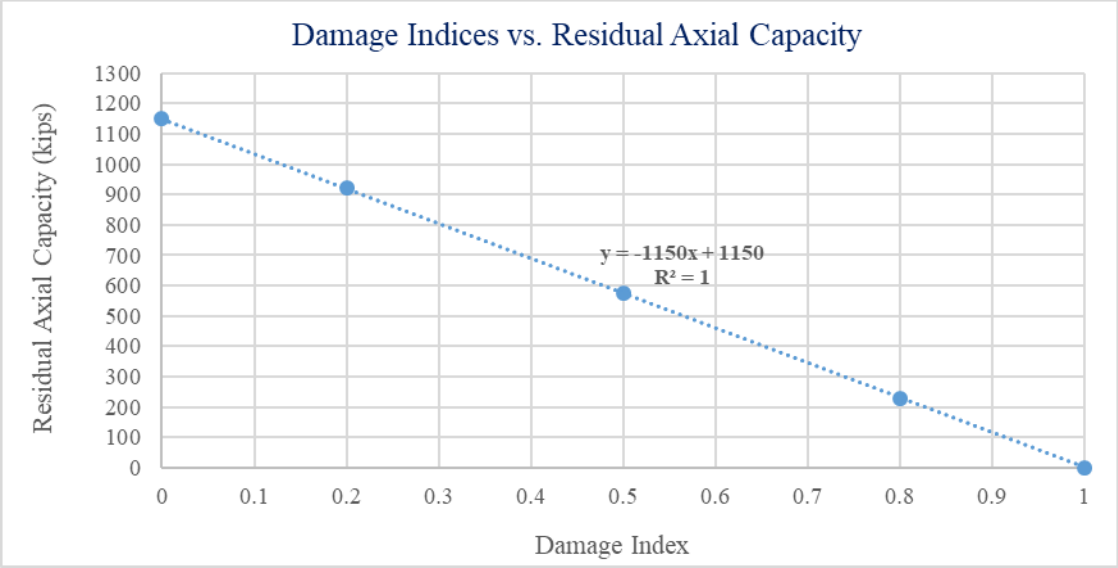

Figure 4-12 Residual Pier Capacity with the Corresponding Damage Indices

4.5 Conclusions

This research is an attempt to provide an insight on recognizing the severity of damage for vehicle impacted piers in different scenarios. Assessment of the damaged pier and its behavior in terms of severity of damage has been explained and a process for estimating the damage demonstrated. From the results, it is expected that increasing the steel ratio, reducing the pitch of the transverse reinforcement and using a higher grade concrete along with larger pier diameter will help the pier better resist vehicular impact. Furthermore, it is also expected that the pier will perform better against dynamic shear if the shear reinforcement diameter is increased in order to reach higher steel grade. Finally, a relationship between damage indices and residual capacity of the pier has been established and can be used to better analyze the damage and corresponding condition of the damaged pier.

CHAPTER 5 Conclusions

5.1 Summary of Conclusions

Using a standard pier detail utilized by the Utah Department of Transportation, existing methods available in the literature are used to evaluate the damage indices and to compare those results to safety factors in current design codes. The reliability of the pier section is then determined as a function of material properties, geometry, vehicle mass, and vehicle impact velocity. Using numerical analysis techniques, the pier is also analyzed to determine the residual axial and shear capacity post-impact. Finally, the residual capacity is used to determine reduction factors that correlate to damage indices that can be used in future evaluation.

The results of the analysis show that current design codes are non-conservative for vehicle impact design especially for large mass vehicles such as semi-tractor trailers. Results from the reliability analysis indicate probabilities of failure of the pier ranging from 45% to 80% for a vehicle at different velocities from 25 mph to 80 mph. Sensitivity analyses are undertaken to understand the relationship between the individual design variables and the corresponding reliability. Results show that increasing the diameter of the pier without changing other design parameters will result in a lower reliability index and higher probability of failure for the pier. The opposite is true for changing the transverse reinforcement while keeping other parameters unchanged. The underlying relationship between the external and core diameters is also explored to understand how the relationship between these variables affect the system reliability.

From the results of the residual capacity analysis, it is determined that increasing the steel ratio, reducing the pitch of the transverse reinforcement and using a higher grade concrete along with larger pier diameter will help the pier better resist vehicular impact. Furthermore, it is also expected that the pier will perform better against dynamic shear if the shear reinforcement

diameter is increased in order to reach higher steel grade. Finally, a relationship between damage indices and residual capacity of the pier has been established and can be used to better analyze the damage and corresponding condition of the damaged pier. As expected the higher damage index results in lower residual capacity, but surprisingly even low velocity impact that results in minimal damage can dramatically reduce the axial and shear capacity of the pier.

5.2 Future Research

The results of this research demonstrate the need for further analysis of the post impact capacity of reinforced concrete piers. Physical testing is necessary to validate the numerical analysis techniques utilized in this study. Additionally, multi-hazard analysis for the post impacted bridge piers should also be performed. Once this work is completed, the implications to AASHTO design codes should be addressed and the code updated to improve the resilience of bridge piers to multi-hazard loading conditions.

References

AASHTO. (2012). *Bridge Design Specifications*. *American Association of State Highway and Transportation Officials, Washington, DC.*, American Association of State Highway and Transportation Officials …, Washington DC.

AASHTO M145-91. (2008). "AMERICAN ASSOCIATION OF STATE HIGHWAY AND TRANSPORTATION OFFICIALS." *Classification of Soils and Soil-Aggregate Mixtures for Highway Construction Purposes*, 9.

Abdelkarim, O. I., and ElGawady, M. A. (2017). "Performance of bridge piers under vehicle collision." *Engineering Structures*, Elsevier, 140, 337–352.

ACI. (2011). *ACI 318-11: Building Code Requirements for Structural Concrete*. *American Concrete Institute*.

ACI committee 318. (1985). "Building code requirements for structural plain concrete (ACI 318.1-83) and commentary." *International Journal of Cement Composites and Lightweight Concrete*, 7(1), 60.

Agrawal, A. K., Liu, G. Y., and Alampalli, S. (2013). "Effects of truck impacts on bridge piers." *Advanced Materials Research*, Trans Tech Publ, 13–25.

Ameli, M. J., and Pantelides, C. P. (2017). "Seismic analysis of precast concrete bridge columns connected with grouted splice sleeve connectors." *Journal of Structural Engineering*, American Society of Civil Engineers, 143(2), 4016176.

ASCE (2013). "Minimum Design Loads for Buildings and Other Structures (ASCE/SEI 7-10)." American Society of Civil Engineers.

Auyeung, S., Alipour, A., and Saini, D. (2019). “Performance-based design of bridge piers under vehicle collision.” *Engineering Structures*, Elsevier, 191, 752–765.

Baker, W. E., Cox, P. A., Kulesz, J. J., Strehlow, R. A., and Westine, P. S. (2012). *Explosion hazards and evaluation*. Elsevier.

Banthia, N., Mindess, S., Bentur, A., and Pigeon, M. (1989). “Impact testing of concrete using a drop-weight impact machine.” *Experimental Mechanics*, 29(1), 63–69.

Bao, X., and Li, B. (2010). “Residual strength of blast damaged reinforced concrete columns.” *International journal of impact engineering*, Elsevier, 37(3), 295–308.

Bentz, E. C., Vecchio, F. J., and Collins, M. P. (2006). “Simplified modified compression field theory for calculating shear strength of reinforced concrete elements.” *ACI Structural Journal*, 103(4), 614–624.

Bo, X., and Daofan, L. (2011). “Finite element analysis of the collision between ship and bridge pier.” *Ship and Ocean Engineering*, 40(1), 143–151.

Buth, C. E., Brackin, M. S., Williams, W. F., and Fry, G. T. (2011). “Collision Loads on Bridge Piers : Phase 2 . Report of Guidelines for Designing Bridge Piers and Abutments for Vehicle Collisions.” Austin, Texas, 100.

Cao, R., Agrawal, A. K., El-Tawil, S., Xu, X., and Wong, W. (2019). “Heavy Truck Collision with Bridge Piers: Computational Simulation Study.” *Journal of Bridge Engineering*, American Society of Civil Engineers, 24(6), 4019052.

CEN. (2004). “Eurocode 4: design of composite steel and concrete structures - Part 1.1: General rules and rules for buildings.” *European Committee for Standardization*, 1–117.

Chopra, A. K. (n.d.). *Dynamics of Structures, Theory and Applications to Earthquake Engineering*. Upper Saddle River: Pearson-Prentice Hall.

Consolazio, G. R., Cook, R. A., and Lehr, G. B. (2002). *Barge impact testing of the St. George Island causeway bridge. Phase I: feasibility study*.

Consolazio, G. R., Cowan, D. R., Biggs, A., Cook, R. A., Ansley, M., and Bollmann, H. T. (2005). "Full-Scale Experimental Measurement of Barge Impact Loads on Bridge Piers." *Transportation Research Record: Journal of the Transportation Research Board*, 1936(1), 80–93.

Cowper, G., and Symonds, P. (1957). "Strain hardening and strain-rate effects in the impact loading of cantilever beam." *Brown University Division of Applied Mathematics*, 1–46.

Deng, L., and Cai, C. S. (2010). "Development of dynamic impact factor for performance evaluation of existing multi-girder concrete bridges." *Engineering Structures*, 32(1), 21–31.

Deng, L., Wang, W., and Yu, Y. (2015). "State-of-the-art review on the causes and mechanisms of bridge collapse." *Journal of Performance of Constructed Facilities*, American Society of Civil Engineers, 30(2), 4015005.

Ebrahimpour, A., Earles, B. E., Maskey, S., Tangarife, M., and Sorensen, A. D. (2016). *Seismic performance of columns with grouted couplers in Idaho accelerated bridge construction applications*. Idaho. Transportation Dept.

El-Tawil, S., Severino, E., and Fonseca, P. (2005). "Vehicle collision with bridge piers." *Journal of Bridge Engineering*, 10(3), 345–353.

CEN (2002). “1-1: Eurocode 1: Actions on structures–Part 1-1: General actions–Densities, self-weight, imposed loads for buildings.” *European Committee for Standardization*.

Feyerabend, M. (1988). “Hard transverse impacts on steel beams and reinforced concrete beams.” *University of Karlsruhe (TH), Germany*.

Ghee, A. B., Priestley, M. J. N., and Paulay, T. (1989). “Seismic shear strength of circular reinforced concrete columns.” *Structural Journal*, 86(1), 45–59.

Girão Coelho, A. M., Simão, P. D., and Bijlaard, F. S. K. (2012). “Guidance for the design of spliced columns.” *Journal of Structural Engineering*, American Society of Civil Engineers, 138(9), 1079–1088.

Gomez, N. L., and Alipour, A. (2014). “Study of circular reinforced concrete bridge piers subjected to vehicular collisions.” *Structures congress 2014*, 577–587.

Haber, Z. B., Saiidi, M. S., and Sanders, D. H. (2014). “Seismic performance of precast columns with mechanically spliced column-footing connections.” *ACI Structural Journal*, American Concrete Institute, 111(3), 639–650.

He, L.-X., Wu, C., and Li, J. (2019). “Post-earthquake evaluation of damage and residual performance of UHPSFRC piers based on nonlinear model updating.” *Journal of Sound and Vibration*, Elsevier, 448, 53–72.

Hsiao, J. K. (2012). “Bending-Axis Effects on Load-Moment (PM) Interaction Diagrams for Circular Concrete Columns Using a Limited Number of Longitudinal Reinforcing Bars.” *Electronic Journal of Structural Engineering*, EJSE International Ltd., University of Melbourne Grattan St. Parkville VIC …, 12, 1.

Karim, H., Sheikh, M. N., and Hadi, M. N. S. (2014). "Confinement of circular concrete columns: A review." *Proceeding of The 1st International Engineering Conference on Developments in Civil & Computer Engineering Applications (IEC2014)*, 28–36.

Knott, M., and Prucz, Z. (2003). "Vessel collision design of bridges." *Bridge Engineering: Substructure Design*, 9-1-9–18.

Kulkarni, S. M., and Shah, S. P. (1998). "Response of reinforced concrete beams at high strain rates." *ACI Structural Journal*, 95(6), 705–715.

Lam, N. (2017). "A Unified Practical Approach for Estimating the Effects of Rare Dynamic Loading on Structures." *Advances in Structural Engineering and Mechanics*.

Larsen, O. D. (1993). *Ship collision with bridges: The interaction between vessel traffic and bridge structures*. IABSE.

Malvar, L. J. (1998). "Review of static and dynamic properties of steel reinforcing bars." *ACI Materials Journal*.

Malvar, L. J., and Crawford, J. E. (1998). "Dynamic increase factors for steel reinforcing bars [C]." *28th DDESB Seminar. Orlando, USA*.

Mander, J. B., Priestley, M. J., and Park, R. (1988). "Theoretical stress-strain model for confined concrete." *Journal of Structural Engineering (United States)*, 114(8), 1804–1826.

Meir-Dornberg, K. E. (1983). "Ship collisions, safety zones, and loading assumptions for structures in inland waterways." *VDI-Berichte*, 496(1), 1–9.

Michel, K., and Winslow, T. S. (2000). "Cargo ship bunker tanks: Designing to mitigate oil spillage." *Marine Technology and SNAME News*, 37(4), 191–199.

Mohammed, T. A., and Parvin, A. (2013). "Evaluating damage scale model of concrete materials using test data." *Advances in concrete construction*, Techno-Press, 1(4), 289–304.

N. Kishi, O. Nakano, K. G. Matsuoka, and T. A. (2001). "Experimental Study on Ultimate Strength of Flexural-Failure-Type RC Beams under Impact Loading." *Transactions of the 16th International Conference on Structural Mechanics in Reactor Technology*.

Pantelides, C. P., Ameli, M. J., Parks, J. E., and Brown, D. N. (2014). *Seismic evaluation of grouted splice sleeve connections for precast RC bridge piers in ABC*. Utah Department of Transportation.

Priestley, M. J. N., Verma, R., and Xiao, Y. (1994). "Seismic shear strength of reinforced concrete columns." *Journal of Structural Engineering (United States)*, 120(8), 2310–2329.

Rasheed, H. A., Charkas, H., and Melhem, H. (2004). "Simplified Nonlinear Analysis of Strengthened Concrete Beams Based on a Rigorous Approach." *Journal of Structural Engineering*, 130(7), 1087–1096.

Rasheed, H., and Abouelleil, A. (2015). *KDOT Column Expert Ultimate Shear Capacity of Circular Columns using the Simplified Modified Compression Field Theory*. University of Nebraska. Mid-America Transportation Center.

Remennikov, A. M., and Kaewunruen, S. (2007). "Impact resistance of reinforced concrete columns: Experimental studies and design considerations." *Progress in Mechanics of Structures and Materials - Proceedings of the 19th Australasian Conference on the Mechanics of Structures and Materials, ACMSM19*, 817–823.

Saatci, S., and Vecchio, F. J. (2009). “Effects of shear mechanisms on impact behavior of reinforced concrete beams.” *ACI Structural Journal*, 106(1), 78–86.

Sharma, H., Gardoni, P., and Hurlebaus, S. (2014). “Probabilistic demand model and performance-based fragility estimates for RC column subject to vehicle collision.” *Engineering Structures*, 74, 86–95.

Sharma, H., Gardoni, P., and Hurlebaus, S. (2015). “Performance-Based probabilistic capacity models and fragility estimates for RC columns subject to vehicle collision.” *Computer-Aided Civil and Infrastructure Engineering*, 30(7), 555–569.

Sharma, H., Hurlebaus, S., and Gardoni, P. (2012). “Performance-based response evaluation of reinforced concrete columns subject to vehicle impact.” *International Journal of Impact Engineering*, 43, 52–62.

Shi, Y., Hao, H., and Li, Z.-X. (2008). “Numerical derivation of pressure–impulse diagrams for prediction of RC column damage to blast loads.” *International Journal of Impact Engineering*, Elsevier, 35(11), 1213–1227.

“Speeding & Speed Limits Index & Overview.” (n.d.). *www.safeny.ny.gov*.

Standards Association of Australia., Australasian Railway Association., and Austroads. (2004). *Bridge design.* Standards Australia.

Tazarv, M., and Saiidi, M. S. (2016). “Seismic design of bridge columns incorporating mechanical bar splices in plastic hinge regions.” *Engineering Structures*, Elsevier, 124, 507–520.

Thilakarathna, H. M. I., Thambiratnam, D. P., Dhanasekar, M., and Perera, N. (2010). "Numerical simulation of axially loaded concrete columns under transverse impact and vulnerability assessment." *International Journal of Impact Engineering*, Pergamon, 37(11), 1100–1112.

Thomas, R. J., Steel, K., and Sorensen, A. D. (2018). "Reliability analysis of circular reinforced concrete columns subject to sequential vehicular impact and blast loading." *Engineering Structures*, Elsevier, 168, 838–851.

Tsang, H., and Lam, N. T. K. (2008). "Collapse of reinforced concrete column by vehicle impact." *Computer-Aided Civil and Infrastructure Engineering*, Wiley Online Library, 23(6), 427–436.

Vecchio, F. J., and Collins, M. P. (1986). "Modified Compression-Field Theory for Reinforced Concrete Elements Subjected to Shear." *Journal of the American Concrete Institute*, 83(2), 219–231.

Woisin, G. (1979). "Design against Collision." *In: Proc. 3rd International Conference on Collision and groundind of ships*, 27–73.

Zhang, G., Chen, Z., Lu, J., Xu, S., and Zhou, X. (2018). "Experimental study on the impact properties of concrete bridge pier reinforced with stainless steel rebar." *Journal of testing and evaluation*, ASTM International, 46(4), 1650–1658.

Zhou, D., and Li, R. (2018). "Damage assessment of bridge piers subjected to vehicle collision." *Advances in Structural Engineering*, SAGE Publications Sage UK: London, England, 21(15), 2270–2281.

Zhou, D., Li, R., Wang, J., and Guo, C. (2017). “Study on Impact Behavior and Impact Force of Bridge Pier Subjected to Vehicle Collision.” *Shock and Vibration*, 2017, 1–12.